

AD-A194 619



DTIC FILE COPY

AN ANALYSIS OF HEAT TRANSFER
AFTER LOSS OF PRIMARY COOLANT
IN THE SP-100 REACTOR SYSTEM

THESIS

Donald W. Robbins
First Lieutenant, USAF

AFIT/GNE/~~GP~~/88M-8

DEPARTMENT OF THE AIR FORCE
AIR UNIVERSITY

AIR FORCE INSTITUTE OF TECHNOLOGY

Wright-Patterson Air Force Base, Ohio

This document has been approved
for public release and sale; its
distribution is unlimited.

DTIC
ELECTE
JUN 23 1988
S D E

88 6 23 03 8


A194619

REPORT DOCUMENTATION PAGE

Form Approved
OMB No. 0704-0188

1a. REPORT SECURITY CLASSIFICATION UNCLASSIFIED		1b. RESTRICTIVE MARKINGS	
2b. DECLASSIFICATION/DOWNGRADING SCHEDULE		3. DISTRIBUTION/AVAILABILITY OF REPORT Approved for public release; distribution unlimited	
4. PERFORMING ORGANIZATION REPORT NUMBER(S) AFIT/GNE/ENP/88M-8		5. MONITORING ORGANIZATION REPORT NUMBER(S)	
6a. NAME OF PERFORMING ORGANIZATION School of Engineering	6b. OFFICE SYMBOL (if applicable) AFIT/ENP	7a. NAME OF MONITORING ORGANIZATION	
6c. ADDRESS (City, State, and ZIP Code) Air Force Institute of Technology Wright-Patterson AFB, Ohio 45433		7b. ADDRESS (City, State, and ZIP Code)	
8a. NAME OF FUNDING/SPONSORING ORGANIZATION	8b. OFFICE SYMBOL (if applicable)	9. PROCUREMENT INSTRUMENT IDENTIFICATION NUMBER	
8c. ADDRESS (City, State, and ZIP Code)		10. SOURCE OF FUNDING NUMBERS	
		PROGRAM ELEMENT NO.	PROJECT NO.
		TASK NO.	WORK UNIT ACCESSION NO.
11. TITLE (Include Security Classification) See box 19			
12. PERSONAL AUTHOR(S) Donald W. Robbins, 1Lt, USAF			
13a. TYPE OF REPORT MS Thesis	13b. TIME COVERED FROM _____ TO _____	14. DATE OF REPORT (Year, Month, Day) 1988 March	15. PAGE COUNT 72
16. SUPPLEMENTARY NOTATION			
17. COSATI CODES		18. SUBJECT TERMS (Continue on reverse if necessary and identify by block number)	
FIELD	GROUP	SUB-GROUP	
22	02		
		Loss of Coolant Accident, Heat Transfer, Reactor Core Cooling System	
19. ABSTRACT (Continue on reverse if necessary and identify by block number)			
Title: An Analysis of Heat Transfer After Loss of Primary Coolant In the SP-100 Reactor System			
Thesis Chairman: Denis E. Beller, Maj, USAF Assistant Professor of Nuclear Engineering			
<div style="text-align: right;"><i>Approved for public release; LAW AFR 190-1.</i> <i>15 Jun 88</i> D. E. Beller Director for Research and Professional Development Air Force Institute of Technology (AFIT) Wright-Patterson AFB OH 45433</div>			
20. DISTRIBUTION/AVAILABILITY OF ABSTRACT <input checked="" type="checkbox"/> UNCLASSIFIED/UNLIMITED <input type="checkbox"/> SAME AS RPT. <input type="checkbox"/> DTIC USERS		21. ABSTRACT SECURITY CLASSIFICATION UNCLASSIFIED	
22a. NAME OF RESPONSIBLE INDIVIDUAL Denis E. Beller, Maj, USAF		22b. TELEPHONE (Include Area Code) 513-255-4498	22c. OFFICE SYMBOL AFIT/ENP

The purpose of this study was to determine design guidelines for the SP-100 space reactor core cooling system after a loss of coolant accident. SP-100 design parameters were obtained from Los Alamos National Laboratory. The Thermal Systems Analysis Code (TSAP) calculated the temperatures within the fuel assemblies as a result of the fuel decay heat. TSAP is a lumped-parameter network analysis code capable of performing radiative and conductive heat transfer analysis.

The reactor core was assumed to void of coolant instantaneously following a LOCA. The reactor core model consisted of individual fuel pin assemblies containing 36 fuel pins surrounding a central cooling channel. This central cooling channel, or bayonet, is a secondary cooling loop within the reactor core. The bayonet cooling is a safety feature designed to keep the core from reaching temperatures at which the uranium dissociates from the uranium-nitride fuel. TSAP calculated the fuel pin temperatures due to decay heat transient. The performance of the bayonets within a generic reactor core was compared to an actual design. Design guidance was established based on the performance of the bayonets in the generic core. (Theses) 

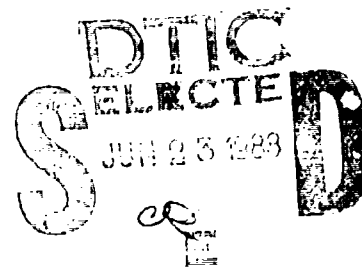
AFIT/GNE/~~ENT~~^{ENT}/88M-8

AN ANALYSIS OF HEAT TRANSFER
AFTER LOSS OF PRIMARY COOLANT
IN THE SP-100 REACTOR SYSTEM

THESIS

Donald W. Robbins
First Lieutenant, USAF

AFIT/GNE/~~ENT~~^{ENT}/88M-8



Approved for public release; distribution unlimited

AFIT/GNE/ENP/88M-8

**AN ANALYSIS OF HEAT TRANSFER
AFTER LOSS OF PRIMARY COOLANT
IN THE SP-100 REACTOR SYSTEM**

THESIS

Presented to the Faculty of the School of Engineering
of the Air Force Institute of Technology

Air University

In Partial Fulfillment of the
Requirements for the Degree of
Master of Science in Nuclear Engineering



Donald W. Robbins, B.NE.
First Lieutenant, USAF

March 1988

Approved for public release; distribution unlimited

Accession For	
NTIS GRA&I	<input checked="" type="checkbox"/>
DTIC TAB	<input type="checkbox"/>
Unannounced	<input type="checkbox"/>
Justification	
By	
Distribution/	
Availability Codes	
Dist	Avail and/or Special

A-1

Preface

The goal of this study was to determine design guidelines for the SP-100 space reactor core cooling system during a loss-of-coolant accident (LOCA). These guidelines were determined by analysis of generic fuel assemblies common to the SP-100 designs. The assemblies, each assembly contains 36 individual fuel pins and one cooling bayonet, were modeled through the use of the TSAP computer program. This procedure identified regions of influence for cooling within each fuel assembly. Once the region of influence is identified for the assemblies, an entire SP-100 reactor core can be analyzed to determine the maximum cooling system necessary to ensure survival of LOCA conditions.

Since this study uses generic design features of the SP-100 reactor core, it may be extended to the competing SP-100 derivative reactor designs. This study is, therefore, an analysis and design tool for continued studies into the SP-100 program.

My appreciation and thanks go to my faculty advisor, Maj D.E. Beller, for his guidance. Also, thanks go to Maj J.A. Lupo for his computer expertise, and to Lt Col R.F. Tuttle for his support and enthusiasm. Special thanks goes to the staff of Los Alamos National Laboratories for sponsoring my work and providing assistance. In particular, I would to thank C. Bell, F. Biehl, J. Elson, and J. Boudreau for their technical guidance and without whose help this work would not have been completed.

Finally, I would like to express my appreciation to my family, Linda, Emily, and Donna, for standing by me and supporting me for the last eighteen months.

Donald W. Robbins

Table of Contents

Preface	ii
List of Figures	v
Abstract	vii
I. Introduction	1.1
Background	1.1
Problem	1.3
Scope	1.3
Assumptions	1.5
Approach	1.6
II. Theory	2.1
Introduction	2.1
Computer Code	2.1
Computer Model	2.3
TSAP Pin-to-Pin Heat Transfer Modeling	2.5
Axial Conduction	2.10
III. Results of the Parametric Investigation	3.1
TSAP Procedures	3.1
Results	3.4
IV. Discussion and Application	4.1
Discussion	4.1
Application	4.2

V. Summary and Recommendations	5.1
Summary	5.1
Recommendations	5.2
Appendix A: SP-100 Design For TSAP Analysis	A.1
Appendix B: TSAP Input File	B.1
Appendix C: Table of Results for the 100 kWe SP-100 from TSAP	C.1
Appendix D: SP-100 3 Safety Rod Configuration	D.1
Appendix E: SP-100 Fission-Product Decay Heat	E.1
Appendix F: Graphical Display of Data	F.1

List of Figures

1.1 Cross-Section of Typical SP-100 Reactor Core	1.4
1.2 Generic Reactor Core Showing Adiabatic Boundary	1.4
2.1 TSAP Model Elements	2.2
2.2 Surfaces of Adjacent Fuel Pins for Conductance Parameter	2.8
3.1 Region of Influence (Rows) vs Linear Power (fuel temp = 1000)	3.2
3.2 Region of Influence (w/cm) vs Linear Power (fuel temp = 1000)	3.2
3.3 Region of Influence (Rows) vs Linear Power (fuel temp = 1000)	3.3
3.3 Region of Influence (w/cm) vs Linear Power (fuel temp = 1000)	3.4
D.1 SP-100 3 Safety Rod Design Temperature Map	D.1
F.1 Region of Influence (Rows) vs Linear Power (fuel temp = 1000)	F.2
F.2 Region of Influence (w/cm) vs Linear Power (fuel temp = 1000)	F.2
F.3 Region of Influence (Rows) vs Linear Power (fuel temp = 1250)	F.3
F.4 Region of Influence (w/cm) vs Linear Power (fuel temp = 1250)	F.3
F.5 Region of Influence (Rows) vs Linear Power (fuel temp = 1400)	F.4
F.6 Region of Influence (w/cm) vs Linear Power (fuel temp = 1400)	F.4
F.7 Region of Influence (Rows) vs Linear Power (fuel temp = 1000)	F.5
F.8 Region of Influence (w/cm) vs Linear Power (fuel temp = 1000)	F.5
F.9 Region of Influence (Rows) vs Linear Power (fuel temp = 1250)	F.6
F.10 Region of Influence (w/cm) vs Linear Power (fuel temp = 1250)	F.6
F.11 Region of Influence (Rows) vs Linear Power (fuel temp = 1400)	F.7
F.12 Region of Influence (w/cm) vs Linear Power (fuel temp = 1400)	F.7

F.13 Region of Influence (Rows) vs Linear Power (fuel temp = 1000)	F.8
F.14 Region of Influence (w/cm) vs Linear Power (fuel temp = 1000)	F.8
F.15 Region of Influence (Rows) vs Linear Power (fuel temp = 1000)	F.9
F.16 Region of Influence (w/cm) vs Linear Power (fuel temp = 1000)	F.9
F.17 Region of Influence (Rows) vs Linear Power (fuel temp = 1000)	F.10
F.18 Region of Influence (w/cm) vs Linear Power (fuel temp = 1000)	F.10
F.19 Region of Influence (Rows) vs Linear Power (fuel temp = 1000)	F.11
F.20 Region of Influence (w/cm) vs Linear Power (fuel temp = 1000)	F.11
F.21 Region of Influence (Rows) vs Linear Power (fuel temp = 1250)	F.12
F.22 Region of Influence (w/cm) vs Linear Power (fuel temp = 1250)	F.12
F.23 Region of Influence (Rows) vs Linear Power (fuel temp = 1250)	F.13
F.24 Region of Influence (w/cm) vs Linear Power (fuel temp = 1250)	F.13
F.25 Region of Influence (Rows) vs Linear Power (fuel temp = 1250)	F.14
F.26 Region of Influence (w/cm) vs Linear Power (fuel temp = 1250)	F.14
F.27 Region of Influence (Rows) vs Linear Power (fuel temp = 1250)	F.15
F.28 Region of Influence (w/cm) vs Linear Power (fuel temp = 1250)	F.15
F.29 Region of Influence (Rows) vs Linear Power (fuel temp = 1400)	F.16
F.30 Region of Influence (w/cm) vs Linear Power (fuel temp = 1400)	F.16
F.31 Region of Influence (Rows) vs Linear Power (fuel temp = 1400)	F.17
F.32 Region of Influence (w/cm) vs Linear Power (fuel temp = 1400)	F.17
F.33 Region of Influence (Rows) vs Linear Power (fuel temp = 1400)	F.18
F.34 Region of Influence (w/cm) vs Linear Power (fuel temp = 1400)	F.18
F.35 Region of Influence (Rows) vs Linear Power (fuel temp = 1400)	F.19
F.36 Region of Influence (w/cm) vs Linear Power (fuel temp = 1400)	F.19

Abstract

The purpose of this study was to determine design guidelines for the SP-100 space reactor core cooling system after a loss-of-coolant accident. SP-100 design parameters were obtained from Los Alamos National Laboratory. The Thermal Systems Analysis Code (TSAP) calculated the temperatures within the fuel assemblies as a result of the fuel decay heat. TSAP is a lumped-parameter network analysis code capable of performing radiative and conductive heat transfer analysis.

The reactor core was assumed to void of coolant instantaneously following a LOCA. The reactor core model consisted of individual fuel pin assemblies containing 36 fuel pins surrounding a central cooling channel. This central cooling channel, or bayonet, is a secondary cooling loop within the reactor core. The bayonet cooling is a safety feature designed to keep the core from reaching temperatures at which the uranium dissociates from the uranium-nitride fuel. TSAP calculated the fuel pin temperatures due to decay heat and identified the maximum temperatures throughout the decay heat transient. The performance of the bayonets within a generic reactor core was compared to an actual design. Design guidance was established based on the performance of the bayonets in the generic core.

AN ANALYSIS OF HEAT TRANSFER AFTER LOSS OF PRIMARY COOLANT IN THE SP-100 REACTOR SYSTEM

I. Introduction

1.1 Background

The Department of Defense (DOD), Department of Energy (DOE), and the National Aeronautics and Space Administration (NASA) are jointly developing space reactor technology (1:232). This technology development is in response to military and civilian space efforts which demand the use of small, durable, high-power systems. Examples of these systems include the Strategic Defense Initiative, space-based radar and navigational systems, and the orbiting space station. The energy requirements of these and future efforts in space require greater power and a longer operational lifetime than is currently available from conventional auxiliary power systems. Currently, the program chartered by the DOD, DOE, and NASA for developing space nuclear power technology is the SP-100 Program (1:232).

Some of the SP-100 Program objectives include (1:232):

1. Ensure aerospace nuclear safety.
2. Define performance limits and satisfy military and civilian applications for space nuclear power.
3. Advance technology in a 100-kilowatt space nuclear power system to support military and civilian missions.
4. Evaluate needs for multimegawatt space nuclear power systems and perform long range technology development efforts.

5. Effectively transition from technology assessment and advancement to engineering development and production for space reactor missions.

The safety issue is one of the biggest problems faced by the SP-100 Program (14). Three phases to the safety issue have been defined by DOE (14). These phases are:

1. During launch.
2. In orbit, during operational mode.
3. In orbit during retirement.

Los Alamos National Laboratory (LANL) is actively involved in assessing the safety of each phase. At this time, LANL believes the most critical safety problem is designing the reactor to withstand a loss-of-coolant accident while it is in orbit (14). General Electric completed a study (8) showing the vulnerability of the SP-100 to impact from meteorites and debris left in orbit from other missions. Impact by debris on the reactor vessel can rupture the vessel wall causing a break in the primary core cooling system. A loss-of-coolant accident (LOCA) can occur when the primary coolant piping breaks and the coolant can't circulate through the core. Even though safety rods reduce the reactor power, there is a continuing supply of heat from decaying fission products in the core. This condition can cause the fuel within the core to increase in temperature until it begins to melt and damages the structural properties of the fuel rods. Once the structural integrity of the reactor is damaged, retiring the system to a high orbit may become difficult. There is also a high probability, after the threshold temperature is exceeded, that molecular uranium will be released in a low earth orbit as the uranium dissociates from the fuel. Therefore, before deployment, a complete thermal analysis must be performed to ensure adequate core cooling after a LOCA.

1.2 Problem

This study will investigate the hypothesis that a generic SP-100 reactor core can be used as a design and analysis tool for other SP-100 designs. Figure 1.1 is a picture of a typical SP-100 reactor core. It is made up of many fuel assemblies and internal structural material. The internal structure gives the core its strength by holding the assemblies in place and adding a conductive heat transfer path.

Figure 1.2 shows a generic fuel assembly totally void of internal structure, except for the fuel cladding.

If the fuel is allowed to melt the internal structure will begin to be attacked by the molten fuel and chemical reaction from free molecular uranium. The uranium dissociates from the uranium-nitride fuel at about 2000 K. By keeping the fuel temperature below 2000 K the core will not melt and the internal structure will remain intact. The problem now becomes one of keeping the core below the threshold temperature.

To understand how to keep the core below the threshold, this study will investigate the behavior of the individual fuel assemblies which make up the core. The assemblies will be void of internal structure and will differ from one another only by the fuel rod linear power. By placing these assemblies in a core configuration, as shown in figure 1.1, the problem of core cooling after a LOCA can be analyzed.

1.3 Scope

This study will be concerned with the SP-100, 100-kilowatt reactor and its derivatives. Specific design features considered are: initial fuel pin temperatures, coolant temperatures, emissivity of the fuel pins, and the fuel linear power. The reactor parameters are given in Appendix A. The Thermal Systems Analysis Program (TSAP) (19) will be used along with the decay heat data in Appendix E to

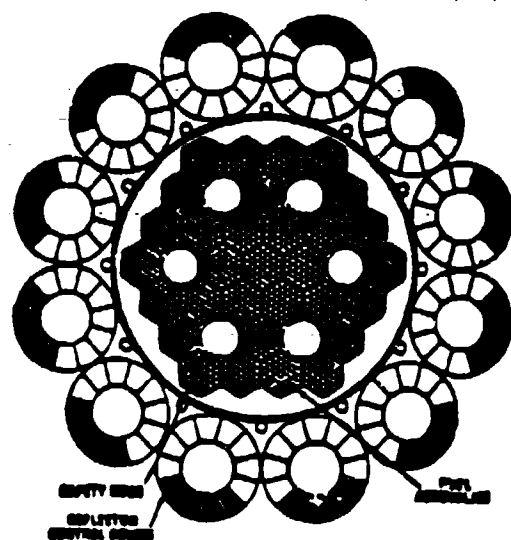


Figure 1.1 Cross-Section of Typical SP-100 Reactor Core (Ref 11)

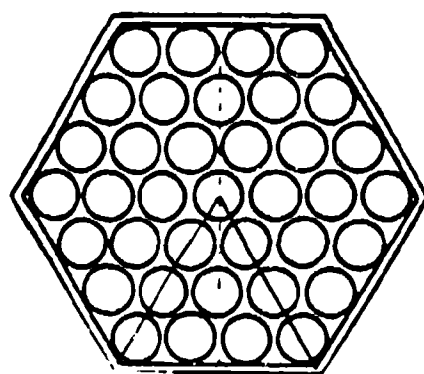


Figure 1.2 Generic Reactor Core Showing Adiabatic Boundary

find the maximum fuel temperature. From the maximum fuel pin temperatures design and analysis guidelines can be devised by considering the regions below the 2000 K threshold, the temperature at which the uranium dissociates from the fuel (16).

The following design parameters will be used along with the data in Appendix A to model the reactor core:

- pin diameter = 0.838 cm
- emissivity of fuel pins = 0.05 - 0.5
- coolant temperature = 800 - 1500 K
- initial fuel pin temperature = 1000 - 1400 K
- fuel pin linear power = 30 - 100 watts/cm

1.4 Assumptions

Assumptions used in this study include:

1. Only a 1-centimeter horizontal slice of the core mid-plane is modeled.
2. Fuel pins are characterized by the initial pin temperature, pin thermal capacitance, and the pin decay heat generation time history.
3. Heat pipes and bayonet cooling rods are modeled by constant temperature only.
4. Heat transfer between fuel pins is radiative.
5. Heat transfer is in the radial direction and negligible in the axial direction.
6. Loss of coolant is instantaneous, with respect to the time scale of the transient coolant loss, and completely voids the core of coolant.

Details concerning these assumptions can be found in the following chapter.

1.5 Approach

The approach of this study is to develop a generic model, void of internal structure, of the SP-100 reactor core. The model will consist of an individual, generic fuel assembly void of conductive heat transfer paths. This assembly will consist of a central bayonet surrounded by hexagonal rows of fuel pins. From the design parameters, changes to the model will be made to determine the effect on the pin temperatures. Data will be taken on the number of fuel pin rows which remain below the 2000 K threshold temperature. This procedure will continue until all the design parameters have been exercised through the ranges of interest defined by LANL.

After accumulating data, the trends indicated by the results will be applied to an SP-100 reactor core design. Design guidance procedures will be developed as the reactor is analyzed using the results from the generic model. In addition, recommendations for future work will be included in the final chapter.

II. Theory

2.1 Introduction

The hypothesis that a generic SP-100 reactor core can be used to determine design guidelines for a complete SP-100 reactor core must be based on basic scientific and engineering principles. This chapter demonstrates those principles used in the analysis of the generic reactor core and allows the application of the data discussed in chapter 3 to any SP-100 configuration with the parameters exhibited in Appendix A.

2.2 Computer Code

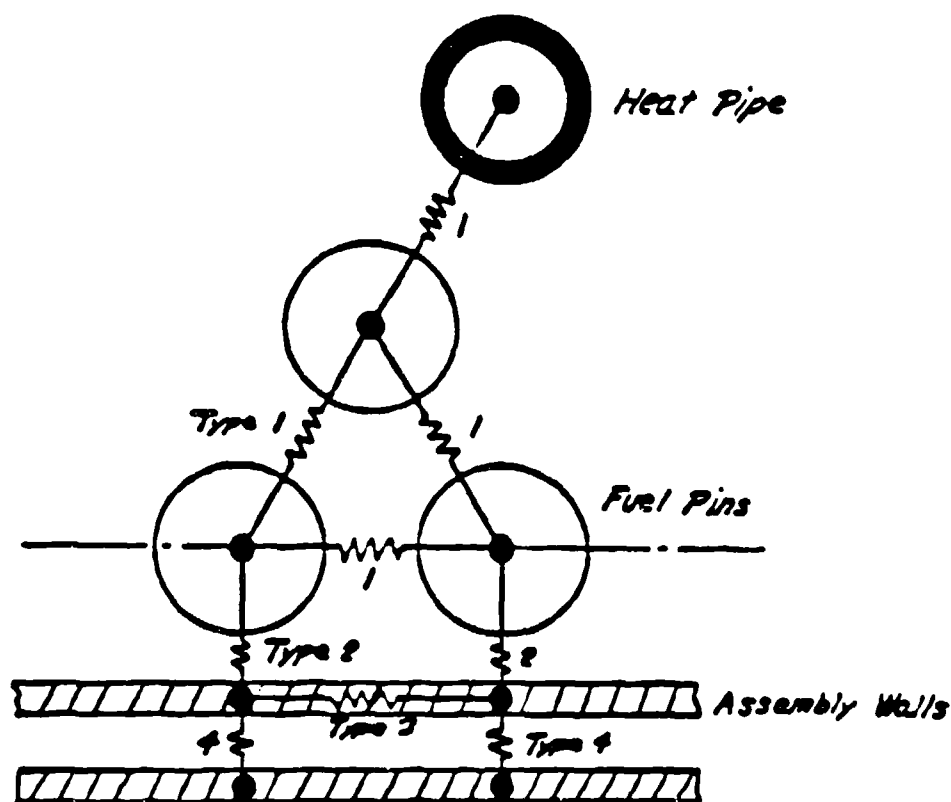
A lumped-parameter computer code called Thermal Systems Analysis Program (TSAP) was used for the calculations. It is a thermal network code which treats the heat transfer as an electrical circuit with the fuel pins and bayonets representing homogeneous nodes (11). Between any two black surfaces 1,2 the radiant heat exchange rate is given by

$$q_{1,2} = A_1 F_{1,2} (E_{b1} - E_{b2}) \quad (2.1)$$

This equation is an analog to Ohm's law, where the quantity of transfer q ; the potential driving force $E_{b1} - E_{b2}$; and the thermal resistance, $\frac{1}{A_1 F_{1,2}}$; have electrical counterparts I , ΔV , and R respectively (2:251). The emissive power of a gray body is given by the Stefan-Boltzmann Law (2:437):

$$E_b = \epsilon \sigma T^4 \quad (2.2)$$

where ϵ represents the emissivity of the surface. Emissivity is a material property and can be determined experimentally. Figure 2.1 shows the typical model elements incorporated in TSAP, and the electrical analog heat transfer paths.



- (a) Fuel pins and assembly walls are characterized by initial temperatures, thermal capacitance, and a heat-generation profile.
- (b) Type 1 and Type 2 conductors are radiative couplers.
- (c) Type 3 conductors are conductive.
- (d) Type 4 conductors are radiative except for a variation in Configuration 4 where they are conductive.
- (e) A heat pipe is characterized by a fixed temperature and a failed heat pipe by a thermal capacitance and an initial temperature.

Figure 2.1 TSAP Model Elements (Ref 11)

2.3 Computer Model

A computer model of a SP-100 reactor core was developed as an input file to TSAP. The model was void of any internal structure, which may have contributed a conductive path in the model; the core contained only fuel pins and bayonet type cooling rods. In order to simplify the analysis, the outer boundary of the model was taken as adiabatic. This results in a 50-100 K higher maximum temperature than the case of allowing the heat to escape into space. However, if the reactor can be cooled at this slightly elevated temperature, it will be within the safety threshold of 2000 K in an operational mode. In addition, the model used (Appendix B) takes advantage of symmetry, so then only one small segment of the reactor core need be modeled. The actual configuration shown in figure 1.2 can be seen to be a subassembly of the fuel pin assemblies shown in figure 1.1.

Appendix B contains all the information necessary for TSAP to calculate the maximum fuel pin temperatures following a LOCA. The "NODE DATA" section contains the data on each individual fuel pin or bayonet node. Bayonet nodes are assumed to be the same size as fuel pins and are actually a generic cooling surface. The bayonet could be a heat pipe, a cold-finger, or any single point cooling mechanism. All operational cooling elements are characterized by the first line contained under the line NODE DATA. The negative sign indicates a constant temperature node, the number 101 is simply a bookkeeping notation for the node number. Bayonet temperature, heat capacity, and linear power complete the input for the bayonet. Since the bayonet is a cooling device, the heat capacity and power level is zero. However, if the bayonet has failed then the model may be changed by removing the negative sign to indicate a node of changing temperature, in this case the bayonet heat capacity must be supplied for TSAP to calculate the temperature change within the bayonet.

Fuel pin data, the lines following the bayonet data, contains the pin number,

the pin initial temperature in degrees kelvin, the fuel pin thermal capacitance in joules per degree kelvin, and the fuel pin linear power in watts per centimeter of pin length. Thermal capacitance is discussed in section 2.4 of this study. Since the fuel pin data is not preceded by a negative sign, the fuel pin temperature is not held constant, and is therefore varied according to the heat transfer paths open to the fuel pin. The heat transfer path data is contained under the "COND DATA" section of the TSAP input file contained in Appendix B.

The heat transfer paths or conduction data can be identified by TSAP as either radiative or conductive. If a conduction data line begins with a negative sign then TSAP used a radiative heat transfer path, if not then a conductive path is used. The first number specifies the conductor identification number, the next two numbers refer to the two nodes the conductor connects. These node numbers refer to the bayonets or fuel pins from the "NODE DATA" section of the input. The last entry in "COND DATA" is the conductance parameter given in watts per degree kelvin to the fourth power. This parameter is discussed in the next section.

The individual nodes and their conductance paths have been defined, now the heat source must be included. For the case of a LOCA the only heat source is the decay heat of the fission-products. The "ARRAY DATA" section includes the time history of the decay heat, and the percent of total thermal power the decay heat represents. The first line is the time entry in seconds, and the second line contains the decay heat data.

Other sections of the TSAP input file include the "CNTL DATA" which specifies time steps for TSAP to use in calculations, and the remainder of the input describes the calculation of the heat flux for use within the TSAP calculations.

2.4 TSAP Pin-to-Pin Heat Transfer Modeling

The TSAP code requires a thermal capacitance input for each node and a thermal conductance input for each conductive path connecting nodes (11). For the thermal capacitance, C , we have:

$$C = \overline{C_p} m \quad (2.3)$$

where

$$m = \overline{\rho} V$$

and

$$\overline{\rho} = \sum_1^n f_i \rho_i$$

$$\overline{C_p} = \frac{\sum_1^n f_i \rho_i c_i}{\overline{\rho}}$$

c_i is the specific heat of material i

$\overline{C_p}$ is the average specific heat of node

f_i is the volume fraction of material i

m is the node mass

V is the node volume

ρ_i is the density of material i

$\overline{\rho}$ is the average density of the node

Therefore, for a fuel pin node the thermal capacitance is

$$C_{pin} = \pi r_{clad}^2 h \left[\left(\rho C_p \right)_{clad} + \left(\rho C_p \right)_{liner} + \left(\rho C_p \right)_{fuel} \right] \quad (2.4)$$

For the bayonet or heat pipe nodes

$$C_b = C_{pb} \rho_b \pi h \left(r_{clad}^2 - r_{ib}^2 \right) \quad (2.5)$$

TSAP uses the conductance, G , between nodes i and j such that

$$q = G \left(T_i - T_j \right) \quad (2.5)$$

for conductive heat transfer, and

$$q = G \left(T_i^4 - T_j^4 \right) \quad (2.6)$$

for radiative heat transfer, where

q is the heat transfer between nodes i and j

T_i is the temperature of node i

T_j is the temperature of node j

The following is a derivation of the conductance parameter G between pins i and j (9). Each pin is assumed to have identical emissivities, thermal conductivities, densities and specific heats. The fuel pins are cylindrical and are positioned in an array on a triangular pitch. Additionally, the pins are assumed infinite in length; each pin is assumed to radiate only to its six nearest neighbors; the interstitial gaps between pins are small compared to some unit fuel pin length, and each pin is represented by a single node and a single temperature (9). This hypothesises that temperature gradients within a given fuel pin are small compared to radiative temperature drops between pins.

Figure 2.2 is used in this derivation to define the surfaces in question. From the figure the heat transfer between i and j is defined as twice the heat from surface 1 to surface 3.

$$q_{i-j} = 2 q_{1-3} \quad (2.7)$$

Assume pin i and pin j have equal temperatures, then the heat transfer between surface 1 and surface 3 is:

$$q_{1-3} = \frac{1}{2} q_{1-2,3} \quad (2.8)$$

Combining equations 2.7 and 2.8 yields

$$q_{i-j} = q_{1-2,3} \quad (2.9)$$

Looking at the expression for two gray bodies that only see each other;

$$q_{1-2,3} = \frac{A_1 \sigma (T_i^4 - T_j^4)}{\left(\frac{1}{\epsilon} - 1 \right) + \frac{1}{F_{1-2,3}} + \frac{A_1}{A_{2,3}} \left(\frac{1}{\epsilon} - 1 \right)} \quad (2.10)$$

where

A_1 is the area of surface 1

$A_{2,3}$ is the area of combined surfaces 2 and 3

$F_{1-2,3}$ is the view factor from surface 1 to the combined surfaces 2 and 3

T_i is the temperature of pin i

T_j is the temperature of pin j

ϵ is the material emissivity

σ is the Stefan-Boltzmann constant

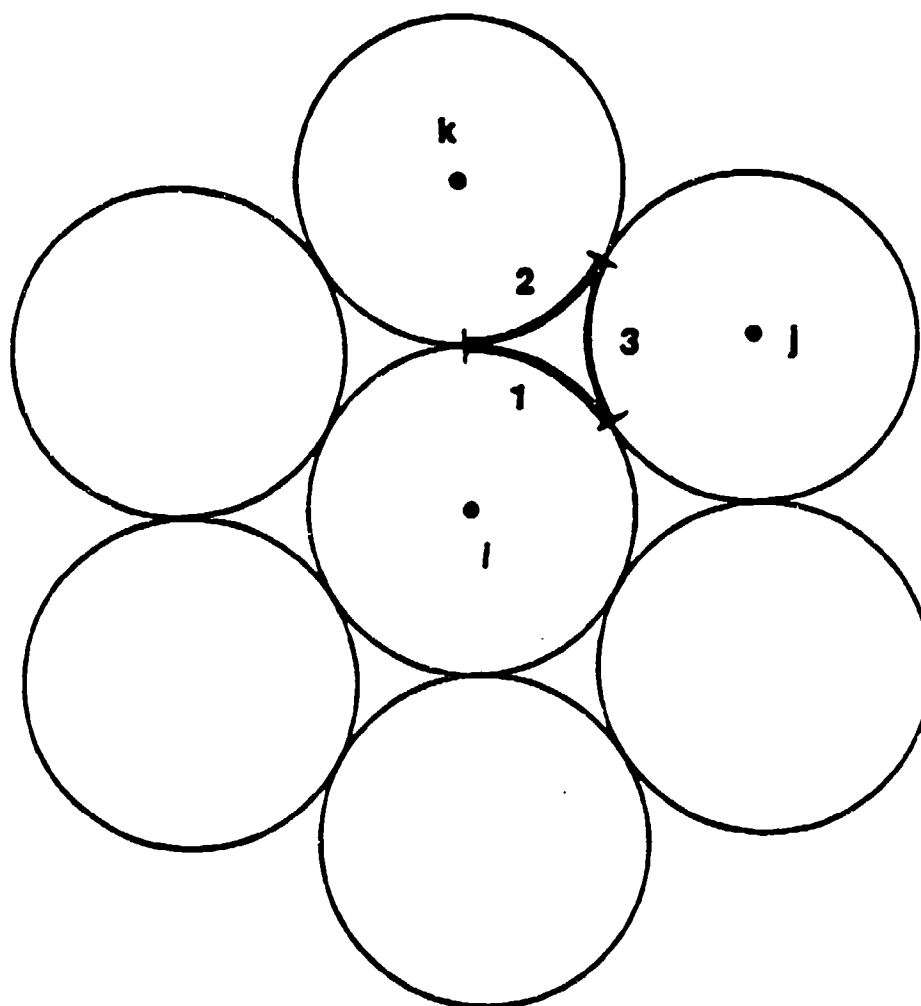


Figure 2.2 Surfaces of Adjacent Fuel Pins for Conductance Parameter (Ref 9)

Combining equations 2.6, 2.9, and 2.10

$$G_{i-j} = A_1 \frac{\sigma}{\left(1 + \frac{A_1}{A_{2,3}}\right) \left(\frac{1}{\epsilon} - 1\right) + \frac{1}{F_{1-2,3}}}$$

From figure 2.2

$$A_1 = \frac{1}{6} \pi D L$$

$$A_{2,3} = 2 A_1$$

$$F_{1-2,3} = 1.0$$

For a fuel pin of diameter D and length L

$$G_{i-j} = \frac{\frac{1}{6} \pi D L \sigma}{\frac{3}{2} \left(\frac{1}{\epsilon} - 1\right) + 1}$$

Simplifying

$$G_{i-j} = \frac{\frac{1}{3} \pi D L \sigma}{\frac{3}{\epsilon} - 1}$$

This expression was derived using the assumption of equal pin temperatures for adjacent pins. Elson in reference 9 derives this equation as a 3-body radiant exchange problem.

2.5 Axial Conduction

Throughout the study, heat transfer in the axial direction has been assumed negligible compared to the radiation heat transfer in the radial direction. To demonstrate that this assumption is valid for reactors of this size, the axial heat transfer and radial heat transfer are compared.

In the axial direction the heat flux rate per rod is found from

$$q = A K \frac{(T_1 - T_2)}{L} \quad (2.11)$$

Where K is the thermal conductivity of the material. The radial heat flux rate per rod is determined by equation 2.10. Using information from Appendix A and reference 18, the axial conductive heat transfer rate per rod is 0.14 watts and the radial radiative heat transfer rate per rod is 27.0 watts. These calculations were based on the smallest temperature difference considered for the SP-100 design, 200 K. This temperature difference minimized the T^4 effect of the radiative heat transfer. When larger changes in temperature are allowed (300- 50 K) the radiative heat transfer rate grows faster than the conductive heat transfer rate.

For this case the ratio of axial conduction versus radial radiation is on the order of 5×10^{-3} . Therefore, neglecting the effect of axial conductive heat transfer by the fuel rods is justified.

III. Results of the Parametric Investigation

3.1 TSAP Procedures

The parameters of emissivity, fuel pin temperature, coolant temperature, and fuel pin linear power were varied over the ranges listed in Chapter I. These values were input into the TSAP code as discussed in Chapter II and in reference 11. A listing of the sample input is in Appendix B.

TSAP uses the node and conduction data to create a thermal map of the reactor core region. The decay heat time history in Appendix E is used to calculate the temperature of each node as the decay heat continues to drop off in time. A new thermal map of the core region is generated for each time step indicated in the input file under the "CNTRL DATA" entries. TSAP will also generate a temperature history of the core region as a function of time, identifying the hottest node within the region and the time at which this temperature occurs. From this updated temperature data, the number of fuel pins remaining below the 2000 K threshold are identified and the number of hexagonal rows containing these pins can be determined. In addition, the total amount of pin linear power cooled by a bayonet, located in the central part of the mapped core region, can be calculated.

Two parameters which are important in a LOCA are the fuel pin emissivity and the coolant temperature in the secondary cooling system. The data displayed on the following graphs are arranged to show cooling trends as one is held constant and the other is varied. Another important parameter in this analysis is the Region of Influence. The features of this parameter are the actual number of hexagonal rows contained in the region and the power (watts/cm) which these rows represent. Figures 3.1 - 3.4 demonstrate these features.

FIXED EMISSIVITY (0.3)

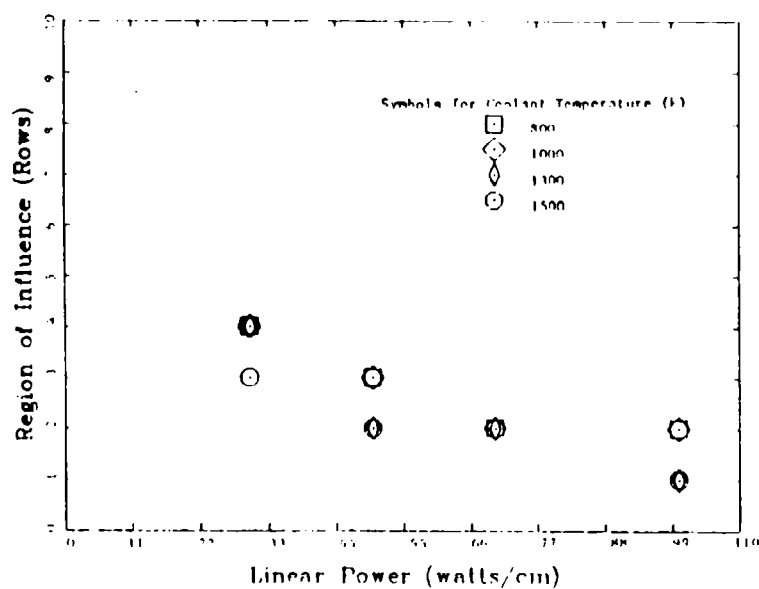


Figure 3.1 Region of Influence (Rows) versus Linear Power (fuel temperature = 1000 K)

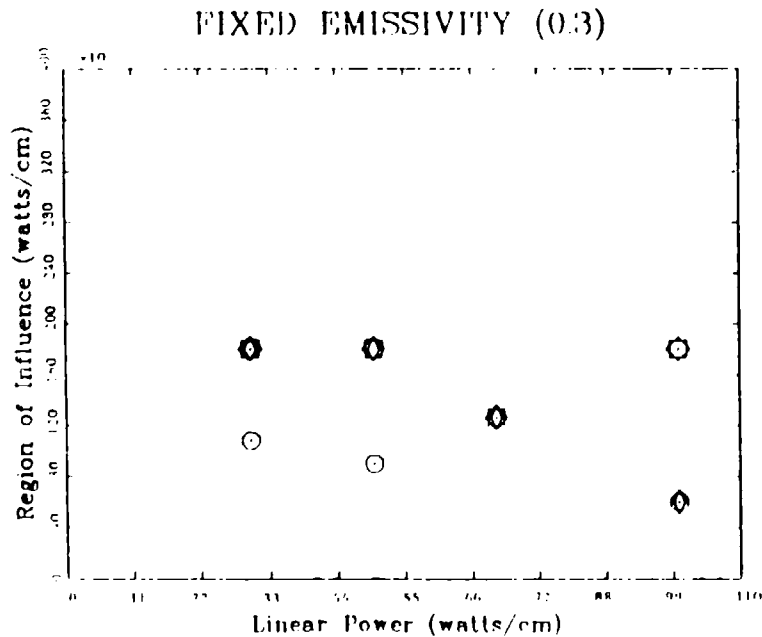


Figure 3.2 Region of Influence (watts/cm) versus Linear Power (fuel Temperature = 1000 K)

FIXED COOLANT TEMPERATURE (800 k)

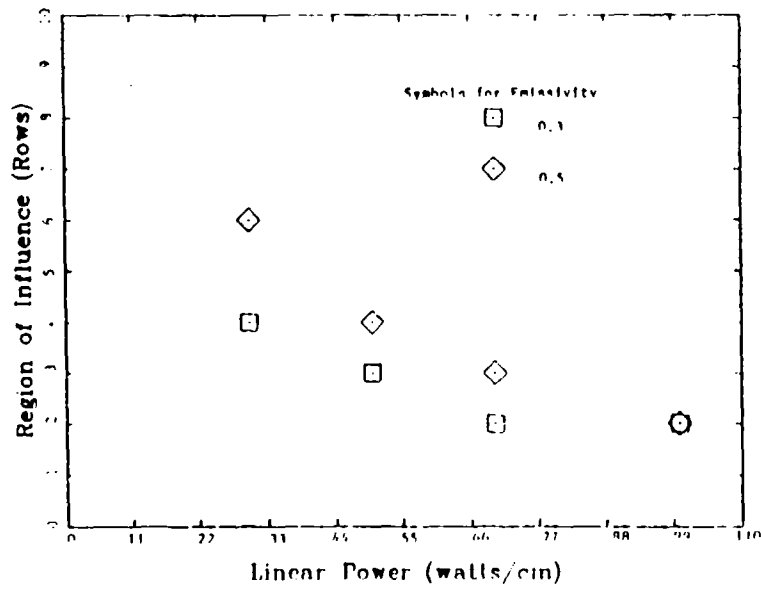


Figure 3.3 Region of Influence (Rows) versus Linear Power (fuel temperature = 1000 K)

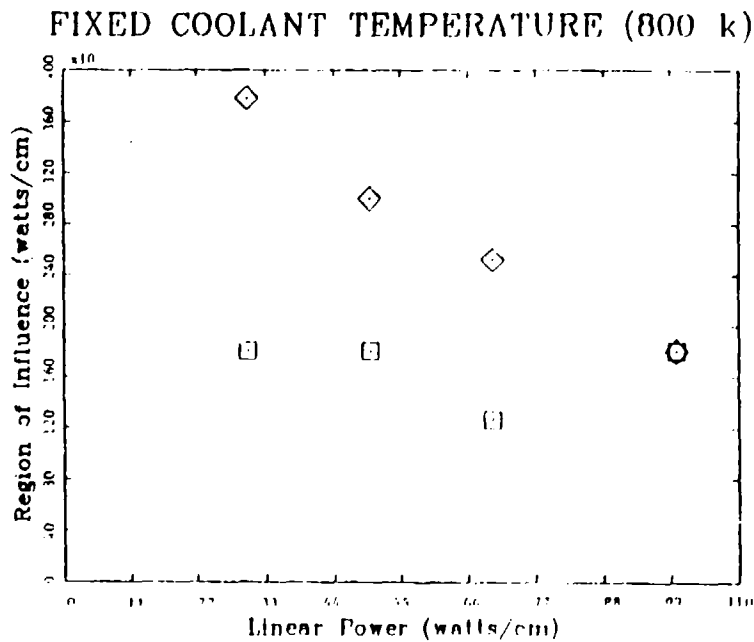


Figure 3.4 Region of Influence (watts/cm) versus Linear Power (fuel temperature = 1000 K)

3.2 Results

Figures 3.1 and 3.2 show the Region of Influence for the case of a fixed emissivity, $\epsilon = 0.3$. Figures 3.3 and 3.4 are fixed at a coolant temperature of 800 K. All of these figures are for a reactor fuel assembly with a fuel pin temperature of 1000 K. The linear fuel pin power is on the x-axis and the Region of Influence is displayed on the y-axis. Symbols for coolant temperature and emissivity on the top graph on each page also hold for the other graph on the page.

For a fixed emissivity, the region of influence, in number of rows cooled, does not change much (1 row) with coolant temperature (700 K) at the same linear power level. However, if the coolant is fixed (800 K) and the emissivity is allowed to vary, the number of rows cooled varies from 4 to 6 at 30 watts/cm to no variation at the 100 watts/cm power region. This demonstrates that if the cladding emissivity changes an additional heat removal mechanism can be gained or lost depending on the change in the emissivity. If the emissivity increases with the fuel pin age, due to roughening effects, an older core has a better chance of surviving a LOCA than a fresh core.

From Figure 3.1 at a fuel pin linear power of 30 watts/cm, for an emissivity of 0.5, a coolant at 800 K will cool 6 hexagonal rows of fuel pins. The assumption here is that the coolant is located at the center of the hexagonal fuel array. At a linear power of 100 watts/cm, the same conditions can only cool 2 hexagonal rows. For systems considering high power densities, the emissivity of the clad is an important parameter to maximize for inherent safety during a LOCA.

Figure 3.4 shows the power contained in the region of influence held under the threshold temperature. The apparent discontinuities are due to the discrete nature of the definition of region of influence. The region of influence assumes a hexagonal heat transfer geometry due to fuel assembly manufacturing and design techniques (15). However, the heat transfer path is not hexagonal in nature.

TSAP produces a map of the temperatures within a given core and the results, not part of this study, indicate a different geometric pattern. The sloping pattern in figure 3.4 indicates that the coolant is capable of cooling at 3780 watts/cm but at 100 watts/cm per pin the same conditions cool only 1800 watts/cm (for $\epsilon = 0.5$). This indicates that the fuel pins in the hexagonal array at 100 watts/cm are probably overcooled.

The remaining graphs are included in Appendix F. Additional data was taken for an emissivity of $\epsilon = 0.05$. At this low emissivity the coolant, at any temperature in the region 800 - 1500 K, could cool at the most 1 row at power levels between 30 - 50 watts/cm. Above this power level all the rods melted regardless of the coolant temperature. If the emissivity drops for any reason (eg., lithium plating), the core will not survive a LOCA under the current designs. This data is included in the tables in Appendix C.

IV. Discussion and Application

4.1 Discussion

The graphs in the previous chapter show a strong dependency on the fuel pin emissivity. In the cases where the initial fuel pin temperature and the coolant temperature are held constant, only the emissivity is allowed to vary for a given power level. Regions of influence for maintaining the core below the threshold value vary considerably for the different power levels. The change in the number of rows cooled, from 2 in the low power regions (30 - 50 watts/cm) to no variation in the high power region (> 50 watts/cm), indicates that high power density cores have an inherent problem with LOCA. The lower coolant temperatures in the bayonets does not relieve the problem.

The graphs of region of influence in terms of linear power cooled show a wide variation. This indicates that the cooling bayonets can cool more fuel pins in a region; however, the region is not hexagonal in geometry. This leads to the assumption that the cooling bayonets are overcooling the fuel pin assemblies.

If a reactor is designed with the cooling bayonets placed in the center of the fuel assemblies, then the number of hexagonal rows expected to remain below the threshold is given by the Regions of Influence (Rows). The Region of Influence (watts/cm) indicate how much linear power the bayonet can support before the threshold is reached. This parameter is a constant for a given bayonet. However, due to the definition of the Region of Influence and the method for allowing row survival the bayonet is capable of cooling a larger region. This region is not hexagonal in geometry.

The method of allowing row survival is based on the criterion that all pins in the row must remain below the 2000 K threshold to be counted. This is based on

the reactor core design criteria and core fabrication techniques. (Fuel assemblies are usually placed in a triangular pitch for neutronic and heat transfer purposes (15)). Since a triangular pitch is used in fabrication the fuel assemblies form hexagonal shapes.

4.2 Application

To demonstrate the design guidance from the graphs a reactor core was chosen from one of the preliminary SP-100 design candidates. A 3-safety-rod configuration was chosen to demonstrate the applicability of the preceding data. The 3-safety-rod design (Appendix D) failed at a temperature of 2507 K. The design features a cooling rod temperature of 800 K, fuel pin temperature of 1320 K, and an emissivity of 0.3. The power varied from 51 watts/cm at the outside edge to 63 watts/cm at the central part of the core. The coolant is allowed to flow around the safety rod and is maintained at a constant temperature.

The figures in Appendix F contain data for a reactor with slightly cooler fuel pins (1250 K) but the same emissivity and coolant temperature. From this data, it can be shown that for the given power levels from the graphs, the largest region of influence of the coolant is 2 hexagonal rows of pins. As a result, it can be deduced that this reactor is undercooled after LOCA and will fail. However, if a bayonet is placed at the center of each assembly, the required cooling is achieved. Each fuel assembly contains a central fuel pin surrounded by 36 other pins in a hexagonal array. This establishes a region of influence of 3 for each central pin if that pin were replaced with a bayonet. The reason the reactor achieved a temperature below threshold is due to the conductive paths now available and the overcooling of the pin within the 2 row region of the bayonet.

When the 3-safety-rod model was run, using the cooling system suggested by figure 3.9, the threshold temperature was never achieved (maximum was 1879 K). In addition, the conductive paths within the 3 rod model transferred the heat to

the outside of the core faster and the peak core temperature occurred much later than the decay heat peak.

From this application two important facts become apparent. First, the figures in chapter 3 can be used to quickly gage the appropriate number of cooling bayonets required in each region. Second, conductive paths help the cooling process by driving the peak core temperature to a later time than the decay heat peak temperatures. Since application of the data from figure 3.9 resulted in the core maintaining a temperature of 1879 K instead of 2507 K, the concept of using the generic model is valid. The conductive paths, which are not included in the generic model, act to enhance the cooling.

Further studies need to be performed on the fuel pin materials to determine the effects surface roughness and age have on the emissive properties. If some coolant remains in the pores of the cladding, the emissivity of the fuel cladding will decrease. However, if the fuel cladding becomes rougher with age the emissivity will increase.

V. Summary and Recommendations

5.1 Summary

This study performed a thermal analysis of a SP-100 reactor core, void of all internal structure, after a loss-of-coolant accident. The purpose was to determine the maximum temperatures achieved in a region and to adjust the region so the maximum temperature did not exceed 2000 K, the dissociation temperature of the uranium from the uranium-nitride fuel.

Results of this study produced a set of design graphs which can be applied to determine the initial number of bayonets needed in the cooling system. When applied to a core which initially failed after LOCA due to inadequate cooling; the new cooling system (dictated by the data) enabled the reactor core to maintain temperatures well below the threshold.

The results also indicate a strong dependence on the fuel pin emissivity. This dependence has a stronger influence on the reactor cooling system than the temperature of the coolant. The data in Appendix C and Appendix F show that the coolant temperature may vary as much as 500 K before a difference is noted in the region of influence. However, if the emissivity changes by the same percentage a larger variation can be seen, especially at low power densities.

In addition to the material studies, further work needs to be completed to fill in the graphs in this study. As mentioned earlier, due to the definition of region of influence, the exact behavior between the data points cannot be easily identified. For example, is the region of influence a step function of the power, or is there an empirical relationship somewhere in the data? The answer to this question will greatly enhance the utility of the data in this study.

Overall, the generic design study showed that a successful design can be accomplished using the data obtained. The data in this study will result in overcooling a specific reactor core design due to the nature of the Region of Influence (Rows). Emissivity also plays a major role in the cooling after a LOCA. The exact behavior of the emissivity in the fuel pins can be used to gage the number of bayonets needed to remain below the threshold. Aging and lithium plating are contributing factors to the emissivity changes within the core and have a direct bearing on the emissive properties of the pins.

5.2 Recommendations

As mentioned earlier, the emissivity of the cladding is critical to the heat transfer of the core during a LOCA. Further studies need to be completed on the emissivity changes due to plating and aging. Surface roughness tests should be performed to simulate these effects. The geometric pattern of preferential heat transfer within the fuel assemblies should be studied to determine the extent of overcooling offered by the data presented in this study. Since the hexagonal region of influence results in overcooling the core, a better method of analyzing the heat transfer in the core may be found within the natural heat transfer geometry.

APPENDIX A: SP-100 Design Data For TSAP Analysis

reactor thermal power (W)	= 2.50000e+06
number of fuel pin assemblies	= 3.10000e+01
number of pins per assembly	= 3.70000e+01
core height (m)	= 5.00380e-01
peak-to-average power factor	= 1.44000e+00
fuel pellet outer radius (m)	= 3.20000e-03
fuel/liner gap outer radius (m)	= 3.27500e-03
liner outer radius (m)	= 3.53000e-03
clad outer radius (m)	= 4.19000e-03
fuel density (kg/m ³)	= 1.35140e+04
liner density (kg/m ³)	= 2.10000e+04
clad/structure density (kg/m ³)	= 8.40000e+03
fuel specific heat (J/kgK)	= 2.52000e+02
liner specific heat (J/kgK)	= 1.54000e+02
clad/structure specific heat (J/kgK)	= 2.75000e+02
duct outer flat-to-flat distance (m)	= 5.74500e-02
duct wall thickness (m)	= 1.24500e-03
duct wall conductivity (W/mK)	= 6.56800e+01
heat pipe wall thickness (m)	= 7.00000e-04
axial node height (m)	= 1.00000e-02
clad/structure emissivity	= 3.00000e-01
fuel pin capacitance (J/K)	= 1.64162e+00
heat pipe capacitance (J/K)	= 3.90140e-01
duct half-wall capacitance (J/K)	= 4.66622e-01
peak pin power (W)	= 6.27248e+01
pin-to-pin conductance (W/K ⁴)	= 5.52828e-13
edge pin-to-duct conductance (W/K ⁴)	= 9.85977e-13
corner pin-to-duct conductance (W/K ⁴)	= 7.21244e-13
half duct-to-half duct conductance (rad-W/K ⁴)	= 1.65933e-12
half duct-to-half duct conductance (cond-W/K)	= 4.93064e-02

Figure A.1 SP-100 Design Information (Courtesy LANL)

APPENDIX B: TSAP Input File

AFIT GENERIC REACTOR CORE MODEL (Ti=1000,Tcf=800,P=10,E=.3)
NODE DATA

-101,800.0,0.0,0.0
201,1000.0,0.8208,5.0
301,1000.0,0.8208,5.0
302,1000.0,0.8208,5.0
401,1000.0,1.6415,10.0
402,1000.0,0.8208,5.0
501,1000.0,0.8208,5.0
502,1000.0,1.6415,10.0
503,1000.0,0.8208,5.0
601,1000.0,1.6415,10.0
602,1000.0,1.6415,10.0
603,1000.0,0.8208,5.0
701,1000.0,0.8208,5.0
702,1000.0,1.6415,10.0
703,1000.0,1.6415,10.0
704,1000.0,0.8208,5.0
801,1000.0,1.6415,10.0
802,1000.0,1.6415,10.0
803,1000.0,1.6415,10.0
804,1000.0,0.8208,5.0
901,1000.0,0.8208,5.0
902,1000.0,1.6415,10.0
903,1000.0,1.6415,10.0
904,1000.0,1.6415,10.0
905,1000.0,0.8408,5.0
1001,1000.0,1.6415,10.0
1002,1000.0,1.6415,10.0
1003,1000.0,1.6415,10.0
1004,1000.0,1.6415,10.0
1005,1000.0,0.8408,5.0 ENDD COND DATA

-5001,101,201,2.7642E-13
-5002,201,301,5.5283E-13
-5003,201,302,2.7642E-13
-5004,301,302,5.5283E-13
-5005,301,401,5.5283E-13
-5006,302,401,5.5283E-13
-5007,302,402,2.7642E-13
-5008,401,402,5.5283E-13
-5009,401,501,5.5283E-13
-5010,401,502,5.5283E-13
-5011,402,502,5.5283E-13
-5012,402,503,2.7642E-13
-5013,501,502,5.5283E-13
-5014,502,503,5.5283E-13
-5015,501,601,5.5283E-13
-5016,502,601,5.5283E-13
-5017,502,602,5.5283E-13

-5018,503,602,5.5283E-13
-5019,503,603,2.7642E-13
-5020,601,602,5.5283E-13
-5021,602,603,5.5283E-13
-5022,601,701,5.5283E-13
-5023,601,702,5.5283E-13
-5024,602,702,5.5283E-13
-5025,602,703,5.5283E-13
-5026,603,703,5.5283E-13
-5027,603,704,2.7642E-13
-5028,701,702,5.5283E-13
-5029,702,703,5.5283E-13
-5030,703,704,5.5283E-13
-5031,701,801,5.5283E-13
-5032,702,801,5.5283E-13
-5033,702,802,5.5283E-13
-5034,703,802,5.5283E-13
-5035,703,803,5.5283E-13
-5036,704,803,5.5283E-13
-5037,704,804,2.7642E-13
-5038,801,802,5.5283E-13
-5039,802,803,5.5283E-13
-5040,803,804,5.5283E-13
-5041,801,901,5.5283E-13
-5042,801,902,5.5283E-13
-5043,802,902,5.5283E-13
-5044,802,903,5.5283E-13
-5045,803,903,5.5283E-13
-5046,803,904,5.5283E-13
-5047,804,904,5.5283E-13
-5048,804,905,2.7642E-13
-5049,901,902,5.5283E-13
-5050,902,903,5.5283E-13
-5051,903,904,5.5283E-13
-5052,904,905,5.5283E-13
-5053,901,1001,5.5283E-13
-5054,902,1001,5.5283E-13
-5055,902,1002,5.5283E-13
-5056,903,1002,5.5283E-13
-5057,903,1003,5.5283E-13
-5058,904,1003,5.5283E-13
-5059,904,1004,5.5283E-13
-5060,905,1004,5.5283E-13
-5061,905,1005,2.7642E-13
-5062,1001,1002,5.5283E-13
-5063,1002,1003,5.5283E-13
-5064,1003,1004,5.5283E-13
-5065,1004,1005,5.5283E-13 ENDD CNTL DATA
IPRO,0,
NLOP,5000,
DCNV,0.02,
ISTA,1,
TSTP,10.,
TSTA,0.,


```

TEND,14401.,
TIME,0.,
IVAB,1, ENDD ARRY DATA 1
0.0,60.,600.,3600.,36000.,8.64E+05,8.64E+06,END 2
.0742,.0401,.0247,.0138,.00658,.00256,.000867,END ENDD VAB1 DATA

```

C

```

PER=TERPL1(A1,A2,TIME,TIME,1,1.)
Q201 = 5.000 * PER
Q301 = 5.000 * PER
Q302 = 5.000 * PER
Q401 = 10.000 * PER
Q402 = 5.000 * PER
Q501 = 5.000 * PER
Q502 = 10.000 * PER
Q503 = 5.000 * PER
Q601 = 10.000 * PER
Q602 = 10.000 * PER
Q603 = 5.000 * PER
Q701 = 5.000 * PER
Q702 = 10.000 * PER
Q703 = 10.000 * PER
Q704 = 5.000 * PER
Q801 = 10.000 * PER
Q802 = 10.000 * PER
Q803 = 10.000 * PER
Q804 = 5.000 * PER
Q901 = 5.000 * PER
Q902 = 10.000 * PER
Q903 = 10.000 * PER
Q904 = 10.000 * PER
Q905 = 5.000 * PER
Q1001 = 10.000 * PER
Q1002 = 10.000 * PER
Q1003 = 10.000 * PER
Q1004 = 10.000 * PER
Q1005 = 5.000 * PER ENDD VAB2 DATA

```

C

```

IF(TIME .LT. 7201.)THEN
  ITIME=NINT(TIME)
  IF(ITIME .GT. 3601)THEN
    NPRT=1
  ELSEIF(ITIME .GT. 3599)THEN
    TSTP=3600.
  ELSEIF(ITIME .GT. 1801)THEN
    NPRT=3
  ELSEIF(ITIME .GT. 601)THEN
    NPRT=2
  ELSEIF(ITIME .GT. 599)THEN
    TSTP=600.
  ELSEIF(ITIME .GT. 421)THEN
    NPRT=3
  ELSEIF(ITIME .GT. 301)THEN
    NPRT=2
  ELSEIF(ITIME .GT. 61)THEN

```

```

      NPRT=2
      ELSEIF(ETIME .GT. 50) THEN
        TSTP=60.
      ELSE
        TSTP=10.
        NPRT=3
      ENDIF
    ENDIF
    CALL OUTPUT(NDTOTL,Q,N,TIME,EROR,LOOP,4)
    CALL QFLOW(NDTOTL,NCTOTL,T,G,IZ1,IZ2,IZ3,M,IPRO) ENDD
VAB3 DATA
C ENDD USER DATA
C*****use this statement in vab2 to get output of heat flux at end
C***** of each time step
C*
C*
C*
C*   CALL QFLOW(NDTOTL,NCTOTL,T,G,IZ1,IZ2,IZ3,M,IPRO)
C*
C*
C*
C*****
      SUBROUTINE QFLOW(ND,NC,T,G,IZ1,IZ2,IZ3,M,IPRO)
C
C-----
C
      DIMENSION T(1),G(1),IZ1(1),IZ2(1),IZ3(1),M(1)
      DIMENSION QFLO(30000)
C
      TABS= 0.0
      IF (IPRO .NE. 1) TABS= 0.0
      LACUM=0
      DO 100 I=1,ND
C----- number of conductors connected to node I
        IZ=IZ1(I)
        IF (IZ .EQ. 0) GO TO 100
        IF (IZ .LT. 0) IZ=-IZ
        DO 200 J=1,IZ
          JI=LACUM+J
C----- what node it connects to
          IZP=IZ2(JI)
C----- conductor number - TSAP
          IZG=IZ3(JI)
C----- radiation
          IF (IZG .LT. 0) THEN
            IZG=-IZG
C--- actual conductor number
            TI=T(I)+TABS
            TIZP=T(IZP)+TABS
            QFLO(M(izg))=G(IZG)*(TIZP**4-TI**4)
          ELSE
            QFLO(M(izg))=G(IZG)*(T(IZP)-T(I))
          ENDIF
        ENDIF
      C   type *,'-----'

```

```

C      type *, 'node', JI, 'connects to', IZP, 'with conductor #', m(izg)
C      type *, 't(i) = ', T(i), ' T(izp) = ', T(izp), ' g = ', G(IZG)
C      type *, ' Qflow(' , nog(ji), ') = ', Qflo(nog(ji))
200 CONTINUE
      iacum = iacum + IZ
100 CONTINUE
      WRITE(6,1)
1  FORMAT(//,4X,'*** HEAT FLUX ***')
      WRITE(6,2)(M(I), QFLO(M(I)), I=1, NC)
2  FORMAT(2X,6(1X,I5,2X,E11.4))
      RETURN
      END ENDD ENDD

```

APPENDIX C: Table of Results for the 100 kWe SP-100 from TSAP

	Fuel Pin Temp (k)	Cold Finger Temp (k)	Power (Watts/cm)	Emissivity	# Rows cooled below 2000 k	# Pins cooled below 2000 k	Total pin power cooled below 2000 k (# Pins · Power) w/cm
1	1000	800	30	.05	1	6	180
2				.30	4	60	1800
3				.50	6	126	3780
4			50	.05	1	6	300
5				.30	3	36	1800
6				.50	4	60	3000
7			70	.05	0	0	0
8				.30	2	18	1260
9				.50	3	36	2520
10			100	.05	0	0	0
11				.30	2	18	1800
12				.50	2	18	1800
13	1000	1000	30	.05	1	6	180
14				.30	4	60	1800
15				.50	6	126	3780
16			50	.05	1	6	300
17				.30	3	36	1800
18				.50	4	60	3000
19			70	.05	0	0	0

	Fuel Pin Temp (k)	Cold Finger Temp (k)	Power (Watts/cm)	Emissivity	# Rows cooled below 2000 k	# Pins cooled below 2000 k	Total pin power cooled below 2000 k (# Pins · Power) w/cm
20				.30	2	18	1260
21				.50	3	36	2520
22			100	.05	0	0	0
23				.30	2	18	1800
24				.50	2	18	1800
25	1000	1300	30	.05	1	6	180
26				.30	4	60	1800
27				.50	5	90	2700
28			50	.05	1	6	300
29				.30	2	18	900
30				.50	3	36	1800
31			70	.05	0	0	0
32				.30	2	18	1260
33				.50	3	36	2520
34			100	.05	0	0	0
35				.30	1	6	600
36				.50	2	18	1800
37	1000	1500	30	.05	1	6	180
38				.30	3	36	1080
39				.50	5	90	2700

	Fuel Pin Temp (k)	Cold Finger Temp (k)	Power (Watts/cm)	Emissivity	# Rows cooled below 2000 k	# Pins cooled below 2000 k	Total pin power cooled below 2000 k (# Pins · Power) w/cm
40			50	.05	1	6	300
41				.30	2	18	900
42				.50	3	36	1800
43			70	.05	0	0	0
44				.30	2	18	1260
45				.50	2	18	1260
46			100	.05	0	0	0
47				.30	1	6	600
48				.50	2	18	1800
49	1250	800	30	.05	1	6	180
50				.30	4	60	1800
51				.50	6	126	3780
52			50	.05	1	6	300
53				.30	3	36	1800
54				.50	4	60	3000
55			70	.05	0	0	0
56				.30	2	18	1260
57				.50	3	36	2520
58			100	.05	0	0	0
59				.30	2	18	1800

	Fuel Pin Temp (k)	Cold Finger Temp (k)	Power (Watts/cm)	Emissivity	# Rows cooled below 2000 k	# Pins cooled below 2000 k	Total pin power cooled below 2000 k (# Pins · Power) w/cm
60				.50	2	18	1800
61	1250	1000	30	.05	1	6	180
62				.30	4	60	1800
63				.50	5	90	2700
64			50	.05	1	6	300
65				.30	3	36	1800
66				.50	4	60	3000
67			70	.05	0	0	0
68				.30	2	18	1260
69				.50	3	36	2520
70			100	.05	0	0	0
71				.30	2	18	1800
72				.50	2	18	1800
73	1250	1300	30	.05	1	6	180
74				.30	4	60	1800
75				.50	5	90	2700
76			50	.05	1	6	300
77				.30	2	18	900
78				.50	3	36	1800
79			70	.05	0	0	0

	Fuel Pin Temp (k)	Cold Finger Temp (k)	Power (Watts/cm)	Emissivity	# Rows cooled below 2000 k	# Pins cooled below 2000 k	Total pin power cooled below 2000 k (# Pins · Power) w/cm
80				.30	2	18	1260
81				.50	3	36	2520
82			100	.05	0	0	0
83				.30	1	6	600
84				.50	2	18	1800
85	1250	1500	30	.05	1	6	180
86				.30	3	36	1080
87				.50	4	60	1800
88			50	.05	0	0	0
89				.30	2	18	900
90				.50	3	36	1800
91			70	.05	0	0	0
92				.30	2	18	1260
93				.50	2	18	1260
94			100	.05	0	0	0
95				.30	1	6	600
96				.50	2	18	1800
97	1400	800	30	.05	1	6	180
98				.30	4	60	1800
99				.50	5	90	2700

	Fuel Pin Temp (k)	Cold Finger Temp (k)	Power (Watts/cm)	Emissivity	# Rows cooled below 2000 k	# Pins cooled below 2000 k	Total pin power cooled below 2000 k (# Pins · Power) w/cm
100			50	.05	1	6	300
101				.30	3	36	1800
102				.50	4	60	3000
103			70	.05	0	0	0
104				.30	2	18	1260
105				.50	3	36	2520
106			100	.05	0	0	0
107				.30	2	18	1800
108				.50	2	18	1800
109	1400	1000	30	.05	1	6	180
110				.30	4	60	1800
111				.50	5	90	2700
112			50	.05	1	6	300
113				.30	3	36	1800
114				.50	4	60	3000
115			70	.05	0	0	0
116				.30	2	18	1260
117				.50	3	36	2520
118			100	.05	0	0	0
119				.30	1	6	600

	Fuel Pin Temp (k)	Cold Finger Temp (k)	Power (Watts/cm)	Emissivity	# Rows cooled below 2000 k	# Pins cooled below 2000 k	Total pin power cooled below 2000 k (# Pins · Power) w/cm
120				.50	2	18	1800
121	1400	1300	30	.05	1	6	180
122				.30	3	36	1080
123				.50	4	60	1800
124			50	.05	1	6	300
125				.30	2	18	900
126				.50	3	36	1800
127			70	.05	0	0	0
128				.30	2	18	1260
129				.50	3	36	2520
130			100	.05	0	0	0
131				.30	1	6	600
132				.50	2	18	1800
133	1400	1500	30	.05	1	6	180
134				.30	3	36	1080
135				.50	4	60	1800
136			50	.05	0	0	0
137				.30	2	18	900
138				.50	3	36	1800
139			70	.05	0	0	0

	Fuel Pin Temp (k)	Cold Finger Temp (k)	Power (Watts/cm)	Emissivity	# Rows cooled below 2000 k	# Pins cooled below 2000 k	Total pin power cooled below 2000 k (# pins · Power) w/cm
140				.30	2	18	1260
141				.50	2	18	1260
142			100	.05	0	0	0
143				.30	1	6	600
144				.50	2	18	1800

APPENDIX D: SP-100 3 Safety Rod Configuration

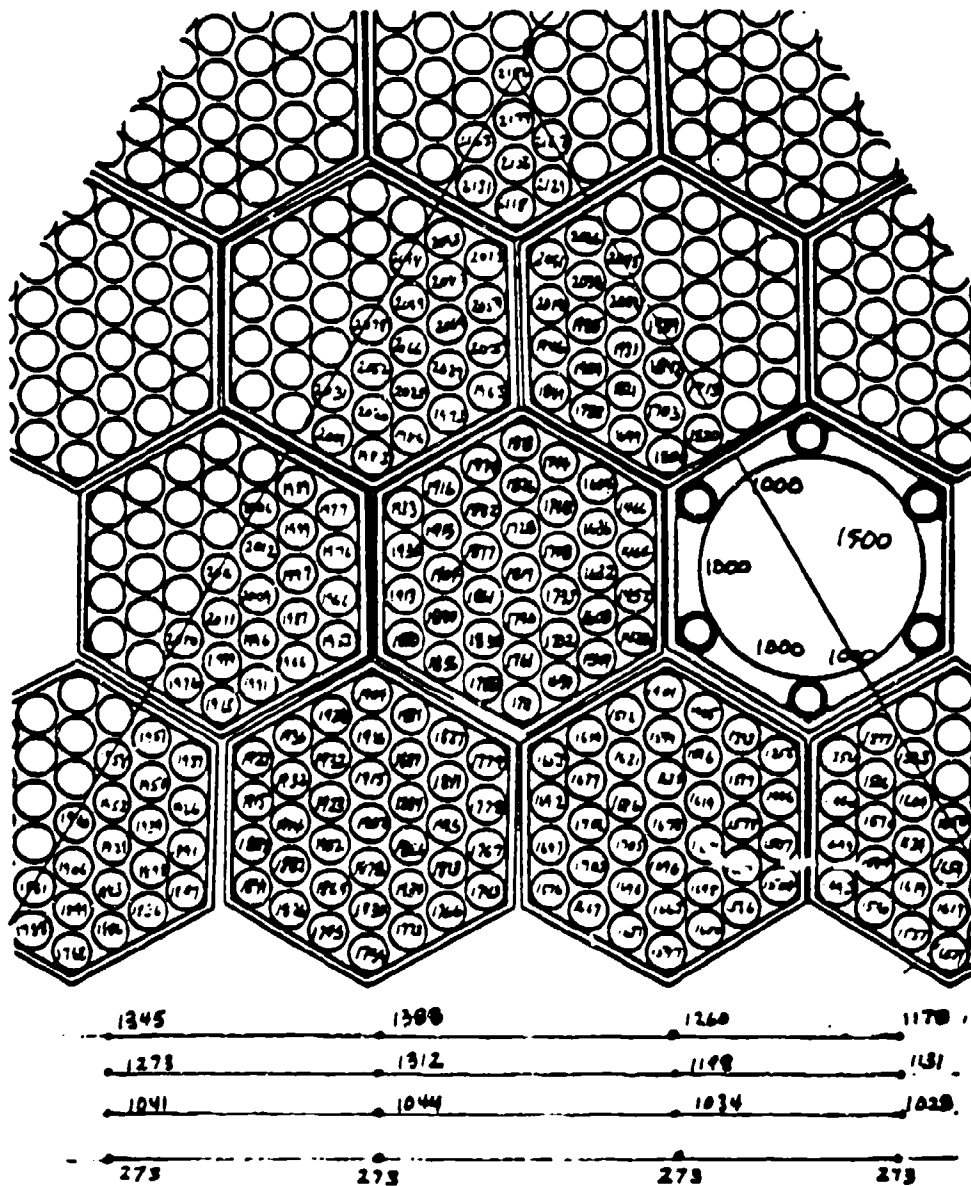


Figure D.1 SP-100 3 Safety Rod Design Temperature Map (Ref 11)

APPENDIX E: SP-100 Fission-Product Decay Heat

<u>Time (Sec)</u>	<u>% Full Power</u>
0.0	7.42
1.0	6.82
2.0	6.49
5.0	5.95
10.0	5.45
20.0	4.90
60.0	4.01
120.0	3.47
300.0	2.86
600.0	2.47
1200.0	1.91
10800.0	1.38
36000.0	0.963
86400.0	0.499
259200.0	0.366
864000.0	0.256
2592000.0	0.164
8640000.0	0.0857
31536000.0	0.0311
94608000.0	0.0128
315360000.0	0.00744

APPENDIX F: Graphical Display of Data

The data presented here is the graphical form of the data in Appendix C except for the exclusion of the data corresponding to an emissivity of 0.05. This data was discussed earlier and contains no useful design information other than to avoid that emissivity. The other curves however, are displayed and should prove useful to reactor designers investigating LOCA conditions.

The symbols represented on the top graph on each page also correspond to the symbols on the bottom of the same page.

FIXED EMISSIVITY (0.3)

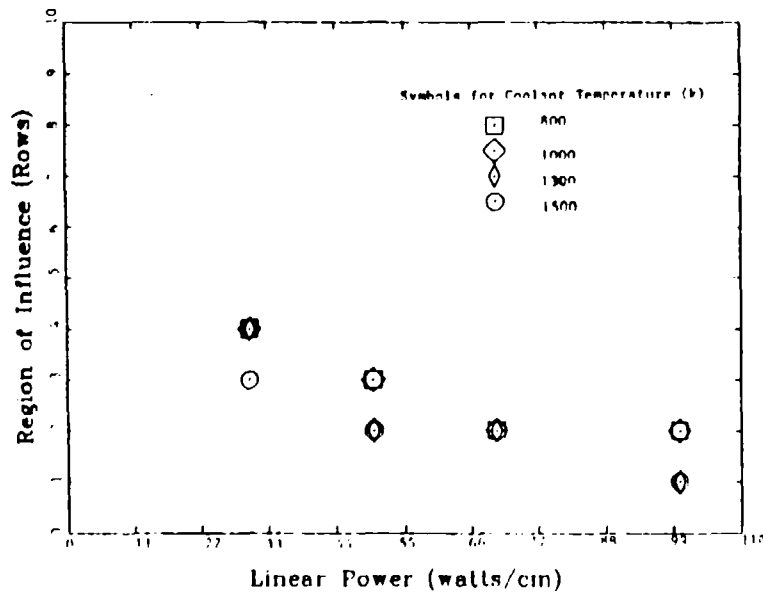


Figure F.1 Region of Influence (Rows) versus Linear Power (fuel temp. = 1000 K)

FIXED EMISSIVITY (0.3)

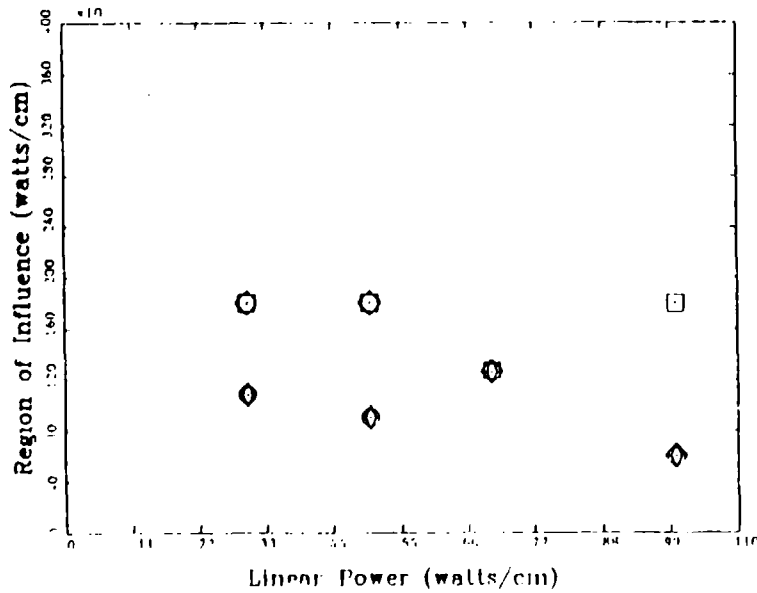


Figure F.2 Region of Influence (W/CM) versus Linear Power (fuel temp. = 1000 K)

FIXED EMISSIVITY (0.3)

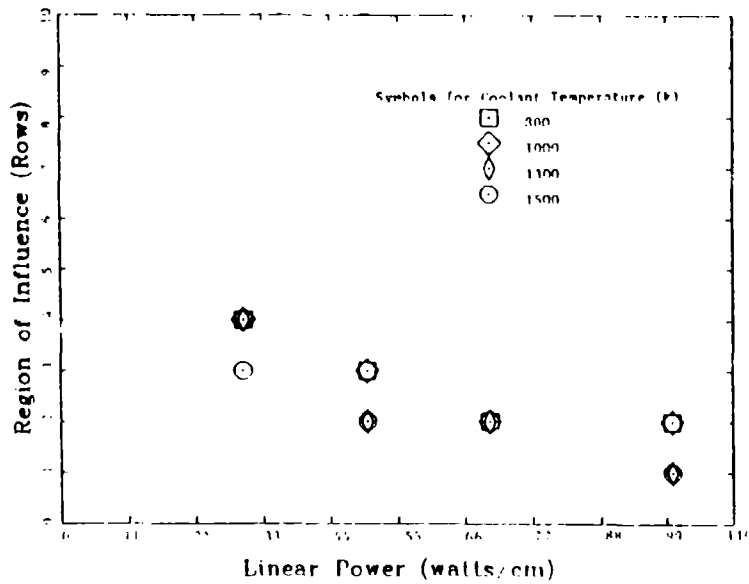


Figure F.3 Region of Influence (Rows) versus Linear Power (fuel temp. = 1250 K)

FIXED EMISSIVITY (0.3)

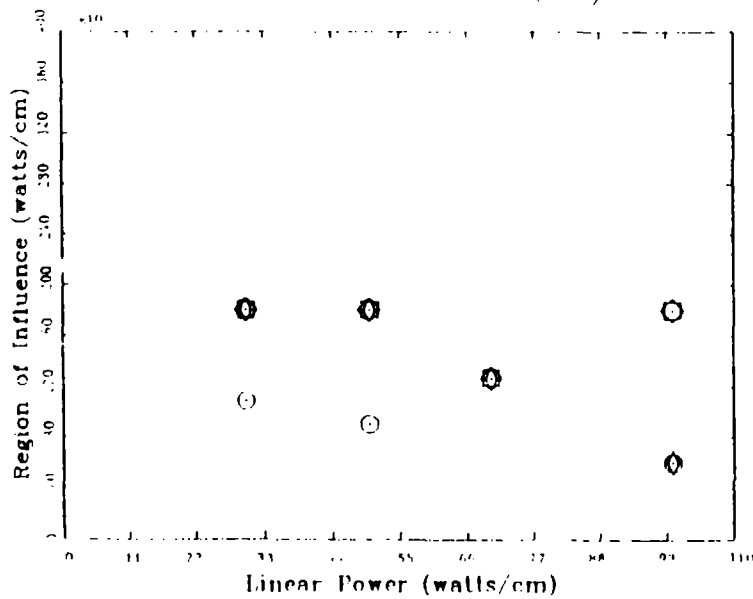


Figure F.4 Region of Influence (W/CM) versus Linear Power (fuel temp. = 1250 K)

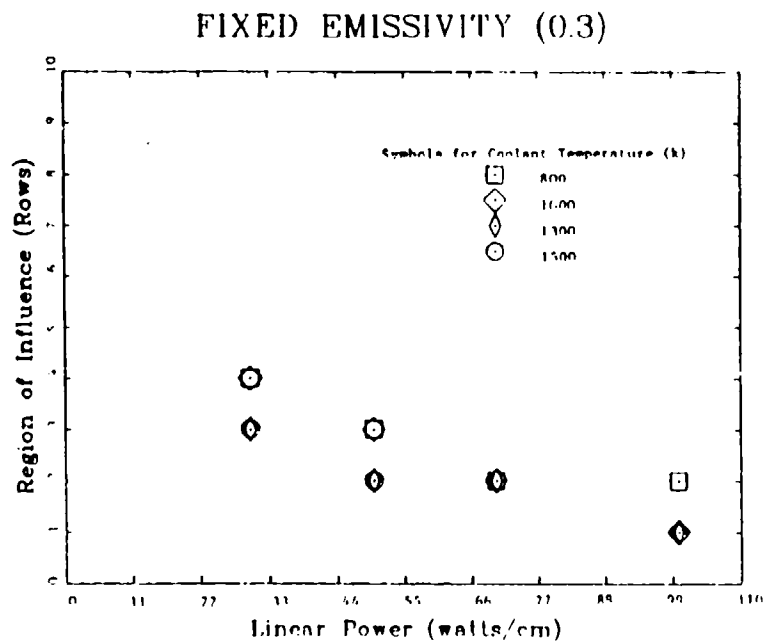


Figure F.5 Region of Influence (Rows) versus Linear Power
(fuel temp. = 1400 K)

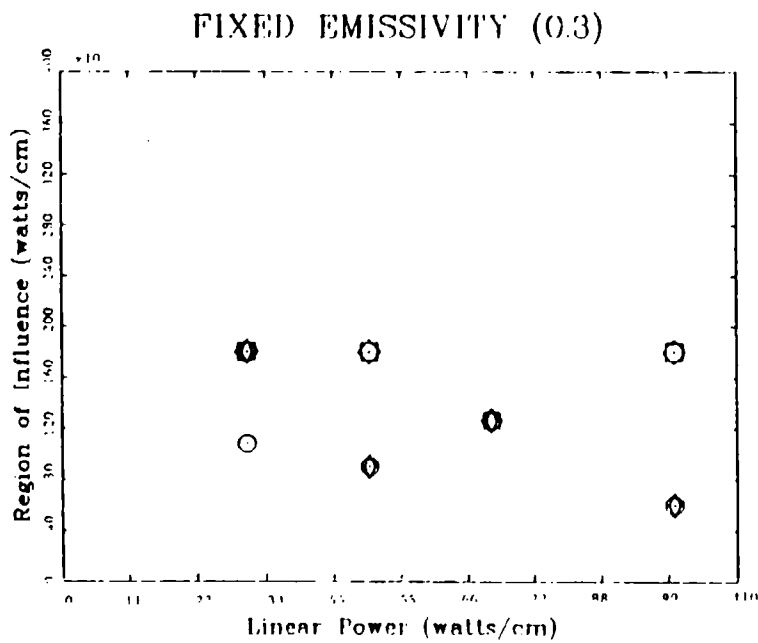


Figure F.6 Region of Influence (W/CM) versus Linear Power
(fuel temp. = 1400 K)

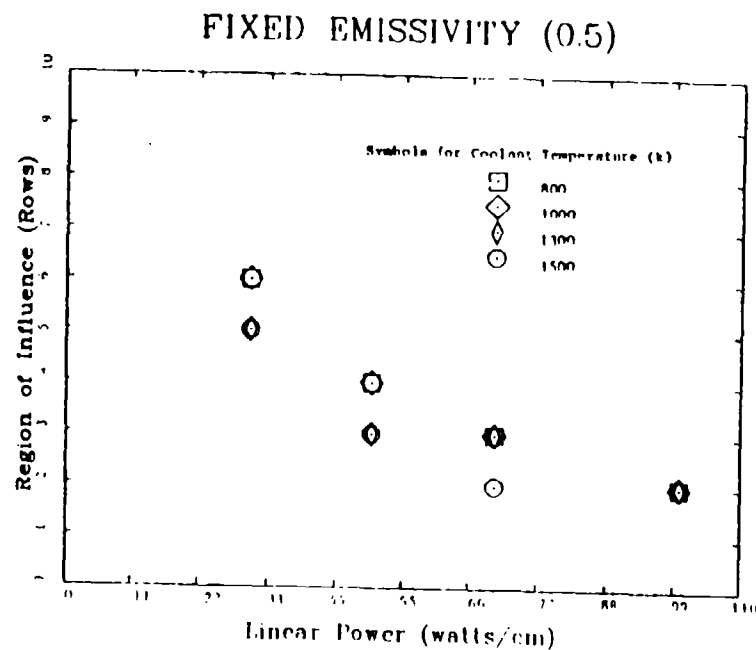


Figure F.7 Region of Influence (Rows) versus Linear Power
(fuel temp. = 1000 K)

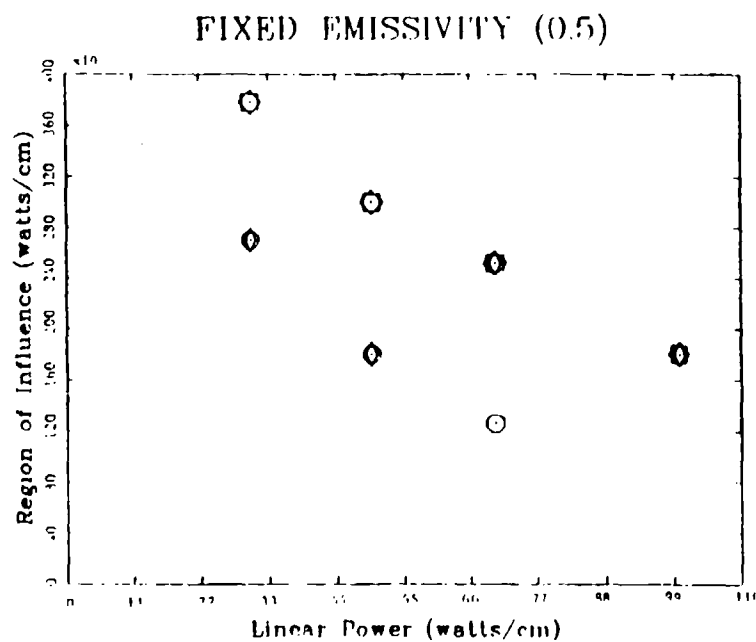


Figure F.8 Region of Influence (W/CM) versus Linear Power
(fuel temp. = 1000 K)

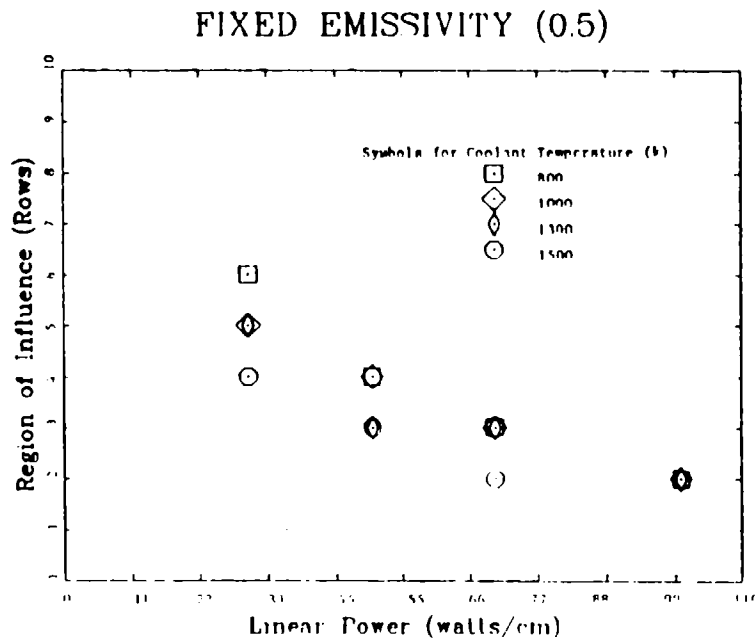


Figure F.9 Region of Influence (Rows) versus Linear Power
(fuel temp. = 1250 K)

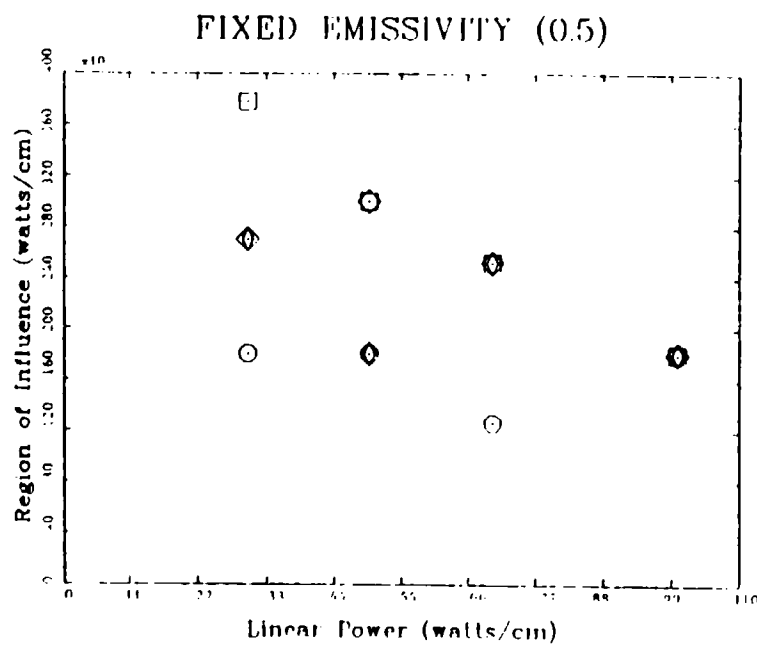


Figure F.10 Region of Influence (W/CM) versus Linear Power
(fuel temp. = 1250 K)

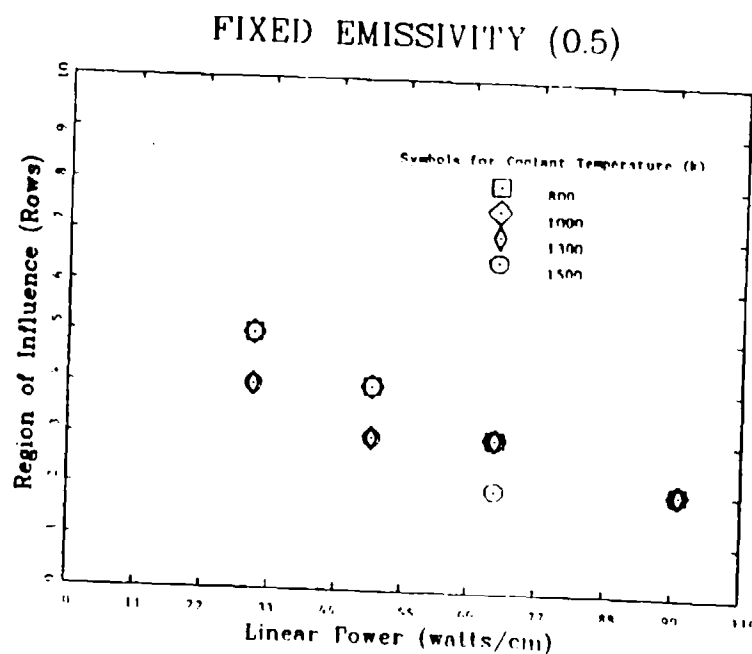


Figure F.11 Region of Influence (Rows) versus Linear Power
(fuel temp. = 1400 K)

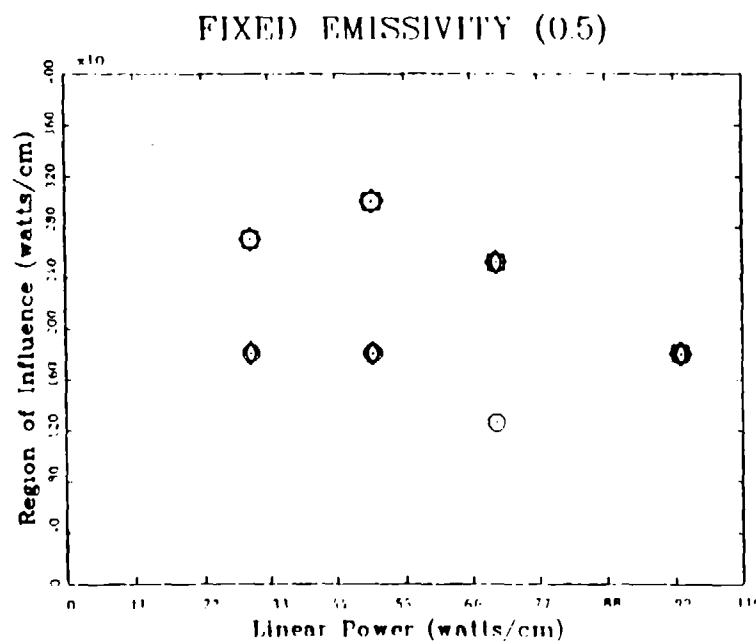


Figure F.12 Region of Influence (W/CM) versus Linear Power
(fuel temp. = 1400 K)

FIXED COOLANT TEMPERATURE (800 k)

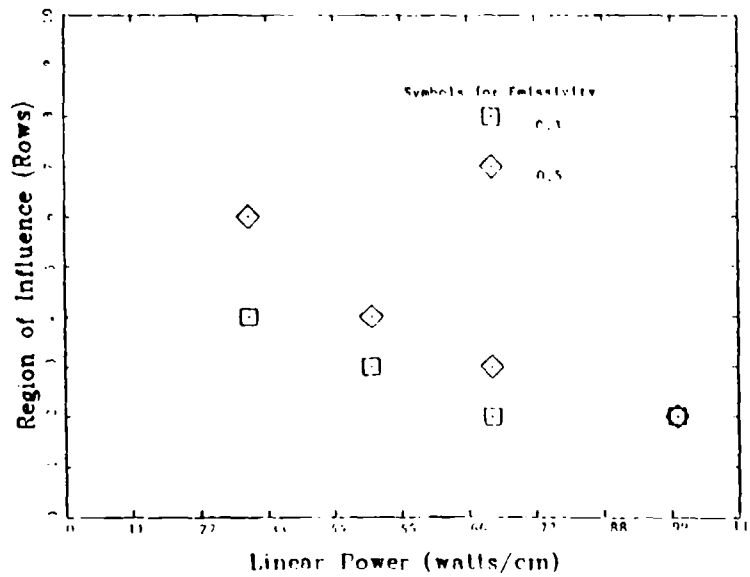


Figure F.13 Region of Influence (Rows) versus Linear Power (fuel temp. = 1000 K)

FIXED COOLANT TEMPERATURE (800 k)

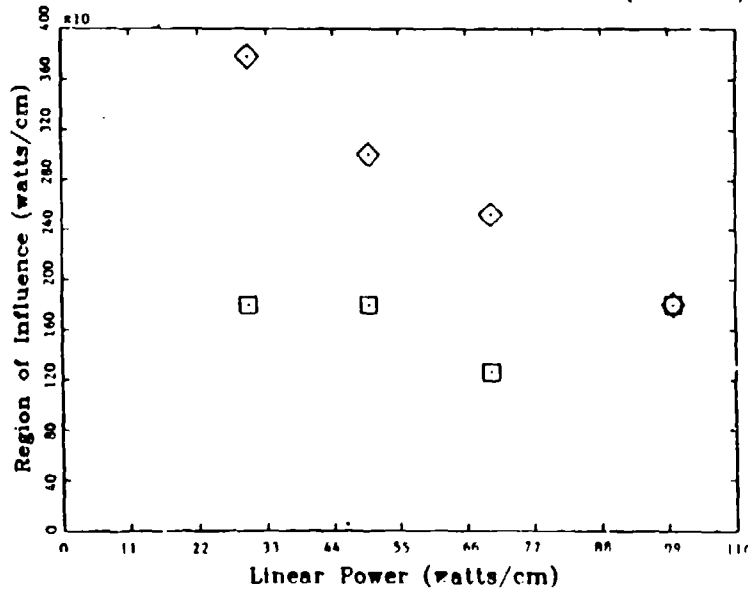


Figure F.14 Region of Influence (W/CM) versus Linear Power (fuel temp. = 1000 K)

FIXED COOLANT TEMPERATURE (1000 k)

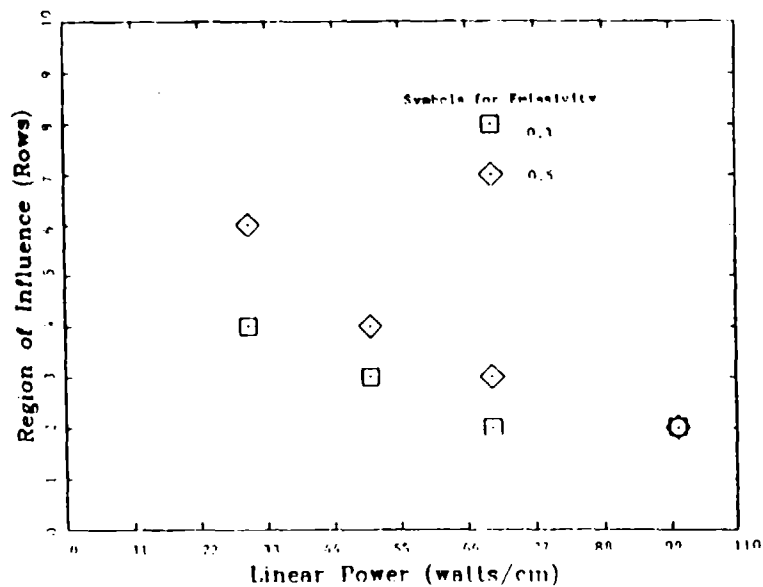


Figure F.15 Region of Influence (Rows) versus Linear Power (fuel temp. = 1000 K)

FIXED COOLANT TEMPERATURE (1000 k)

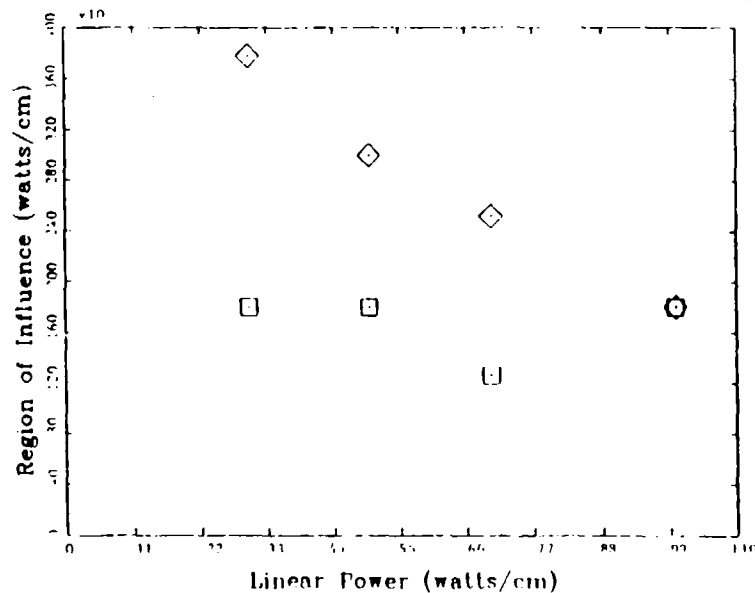


Figure F.16 Region of Influence (W/CM) versus Linear Power (fuel temp. = 1000 K)

FIXED COOLANT TEMPERATURE (1300 k)

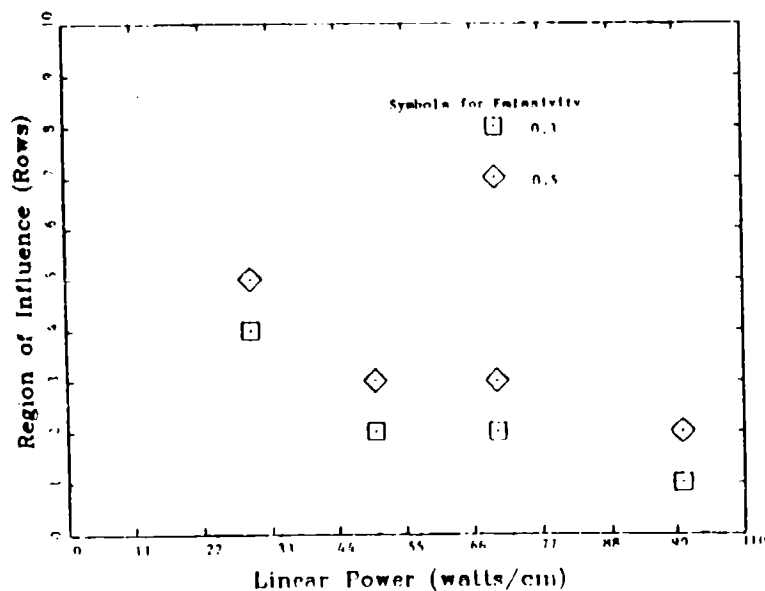


Figure F.17 Region of Influence (Rows) versus Linear Power
(fuel temp. = 1000 K)

FIXED COOLANT TEMPERATURE (1300 k)

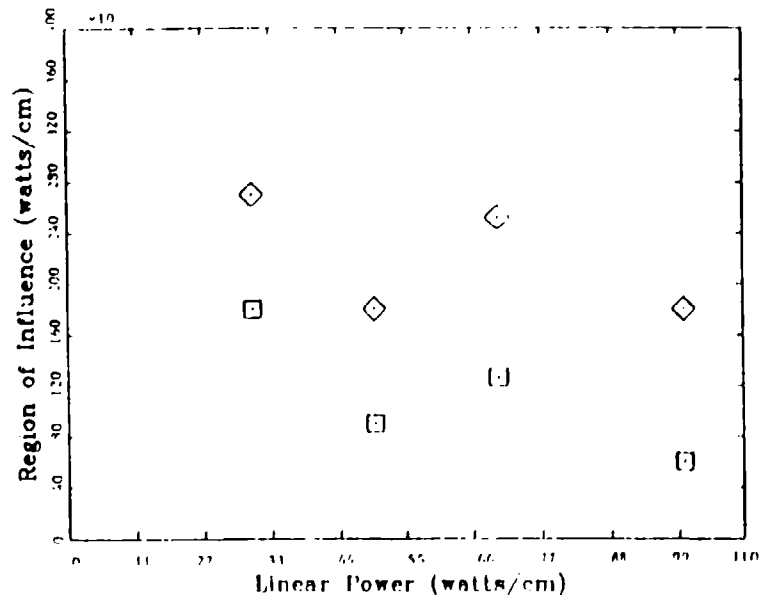


Figure F.18 Region of Influence (W/CM) versus Linear Power
(fuel temp. = 1000 K)

FIXED COOLANT TEMPERATURE (1500 k)

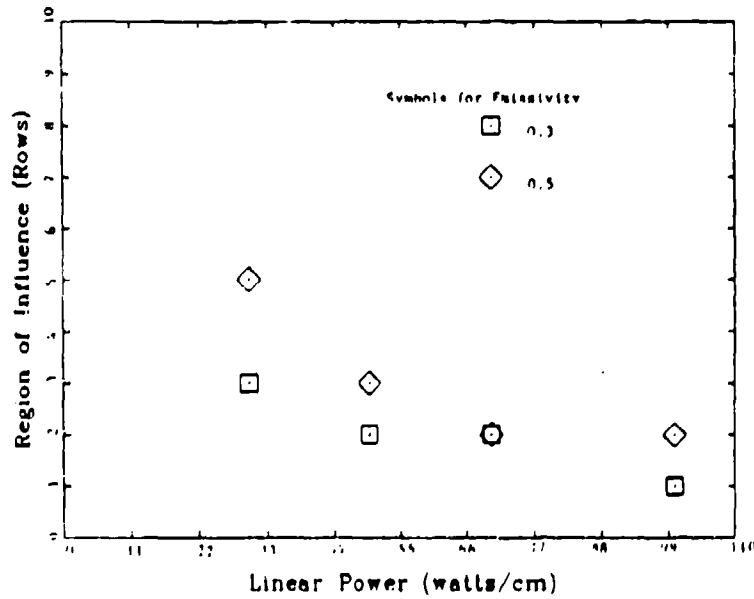


Figure F.10 Region of Influence (Rows) versus Linear Power (fuel temp. = 1000 K)

FIXED COOLANT TEMPERATURE (1500 k)

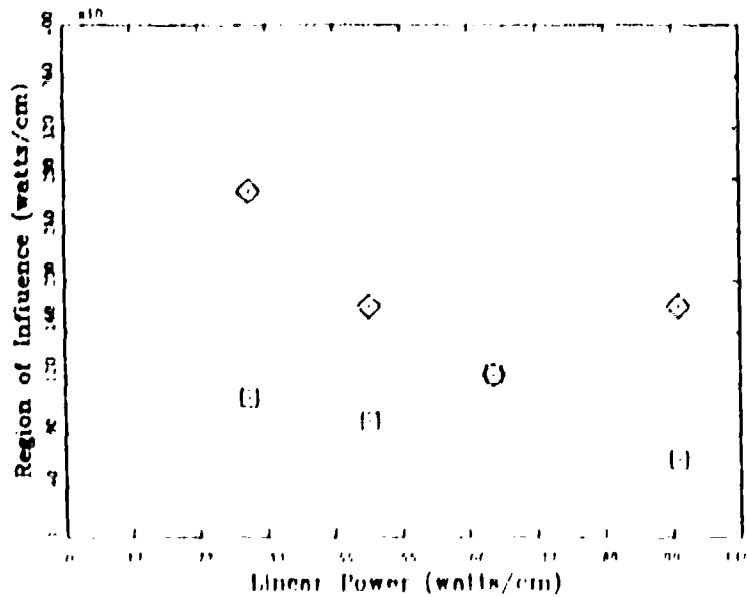


Figure F.20 Region of Influence (W/CM) versus Linear Power (fuel temp. = 1000 K)

FIXED COOLANT TEMPERATURE (800 k)

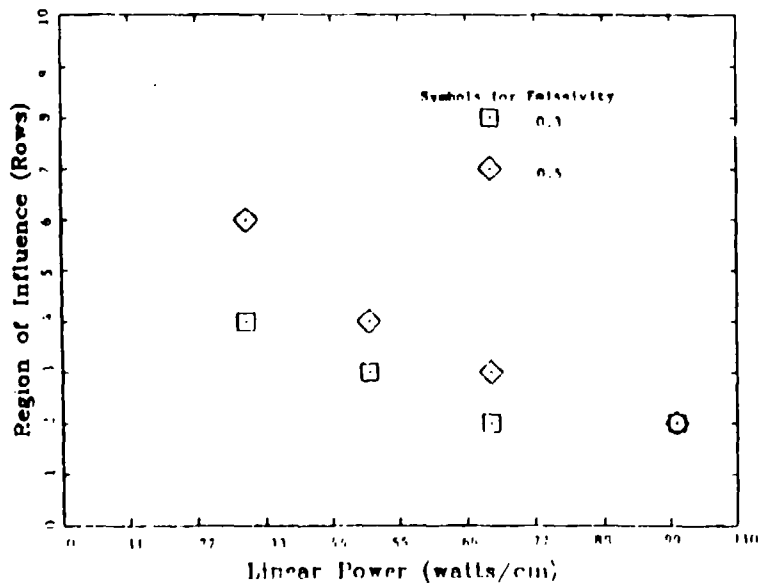


Figure F.21 Region of Influence (Rows) versus Linear Power (fuel temp. = 1250 K)

FIXED COOLANT TEMPERATURE (800 k)

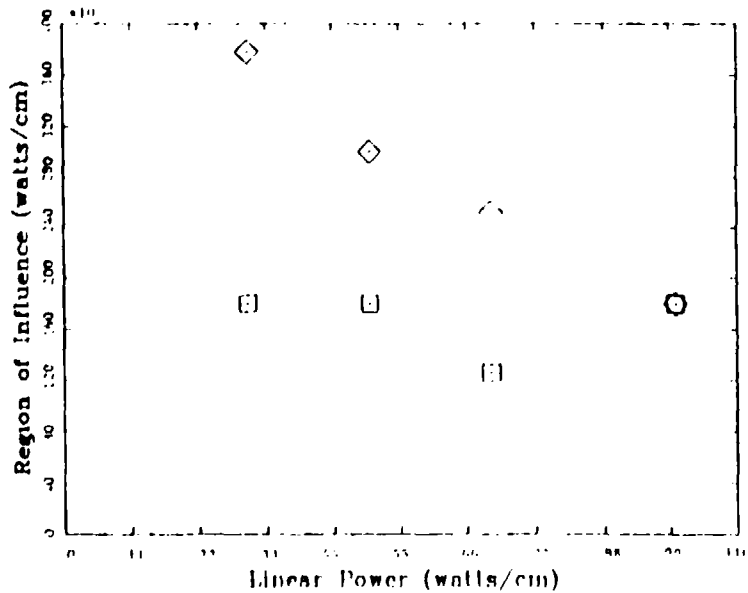


Figure F.22 Region of Influence (W/CM) versus Linear Power (fuel temp. = 1250 K)

FIXED COOLANT TEMPERATURE (1000 k)

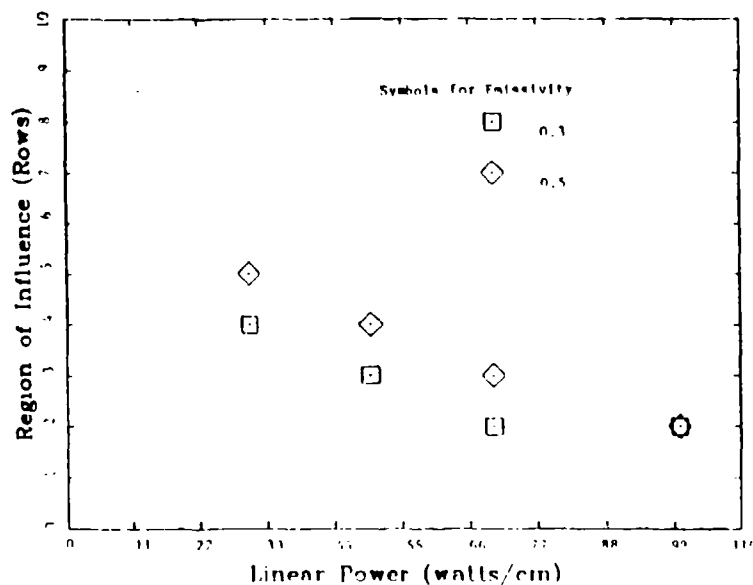


Figure F.23 Region of Influence (Rows) versus Linear Power
(fuel temp. = 1250 K)

FIXED COOLANT TEMPERATURE (1000 k)

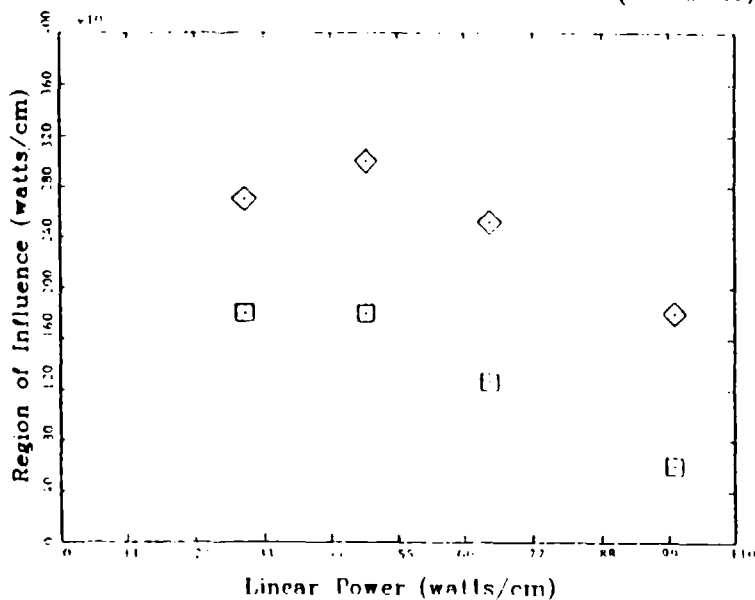


Figure F.24 Region of Influence (W/CM) versus Linear Power
(fuel temp. = 1250 K)

FIXED COOLANT TEMPERATURE (1300 K)

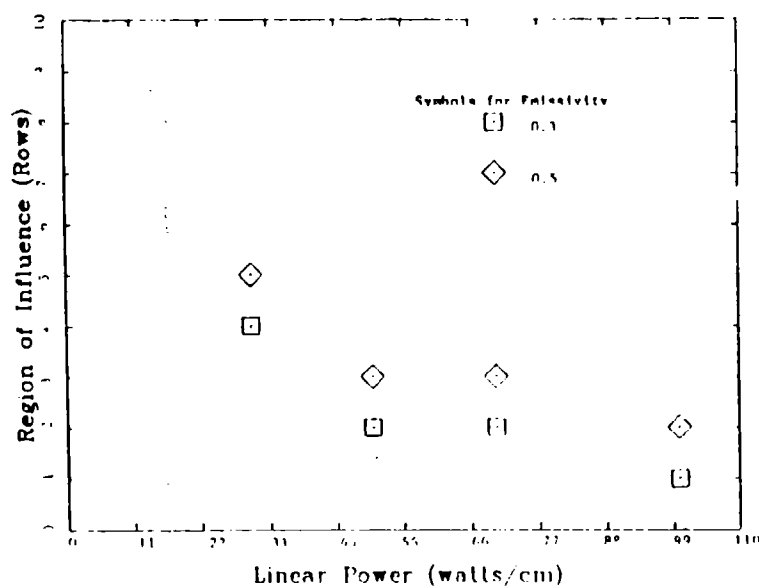


Figure F.25 Region of Influence (Rows) versus Linear Power (fuel temp. = 1250 K)

FIXED COOLANT TEMPERATURE (1300 K)

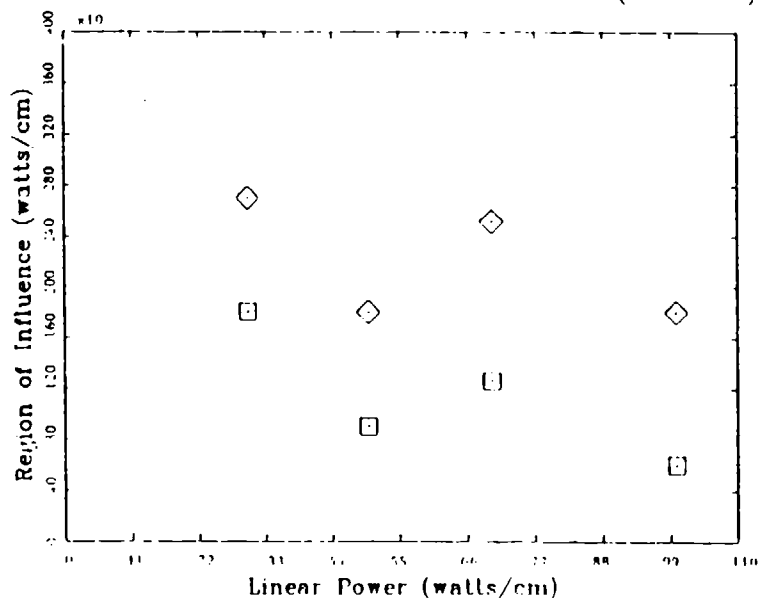


Figure F.26 Region of Influence (W/CM) versus Linear Power (fuel temp. = 1250 K)

FIXED COOLANT TEMPERATURE (1500 K)

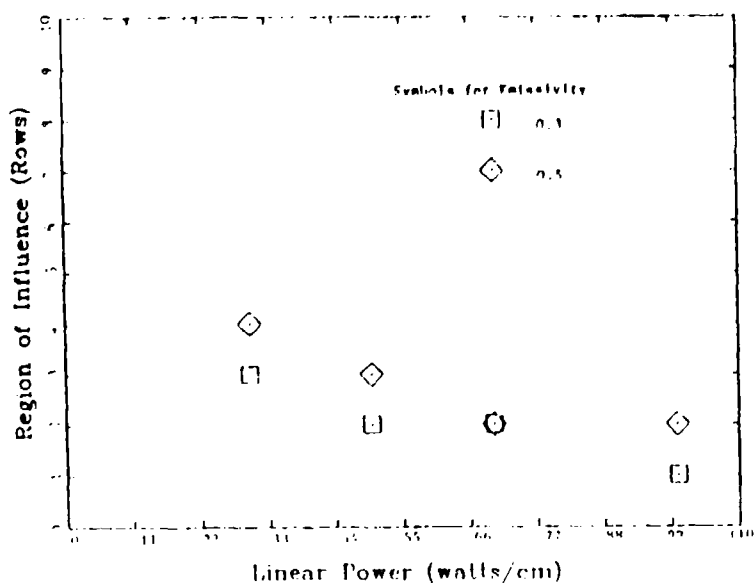


Figure F.27 Region of Influence (Rows) versus Linear Power (fuel temp. = 1250 K)

FIXED COOLANT TEMPERATURE (1500 K)

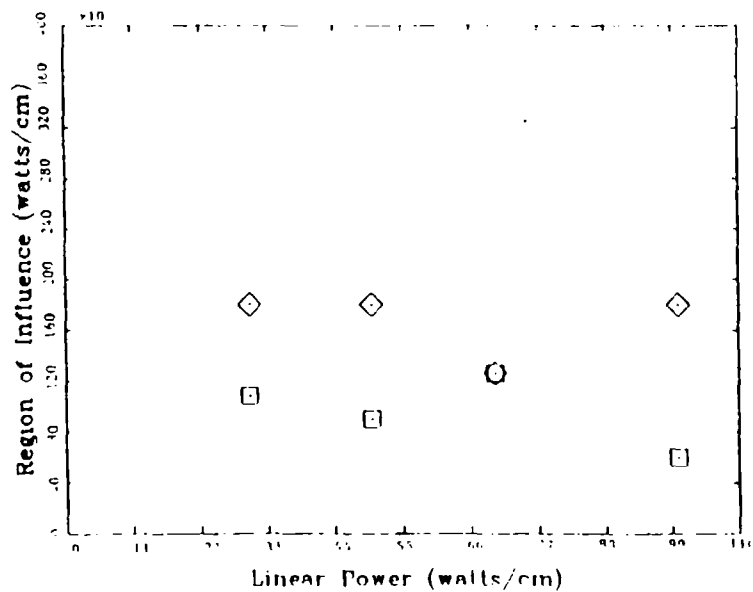


Figure F.28 Region of Influence (W/CM) versus Linear Power (fuel temp. = 1250 K)

FIXED COOLANT TEMPERATURE (800 k)

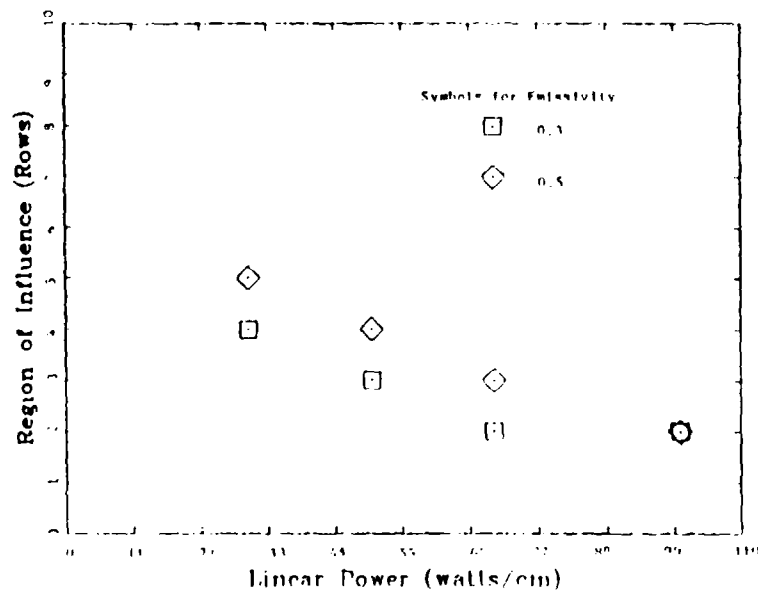


Figure F.29 Region of Influence (Rows) versus Linear Power
(fuel temp. = 1400 K)

FIXED COOLANT TEMPERATURE (800 k)

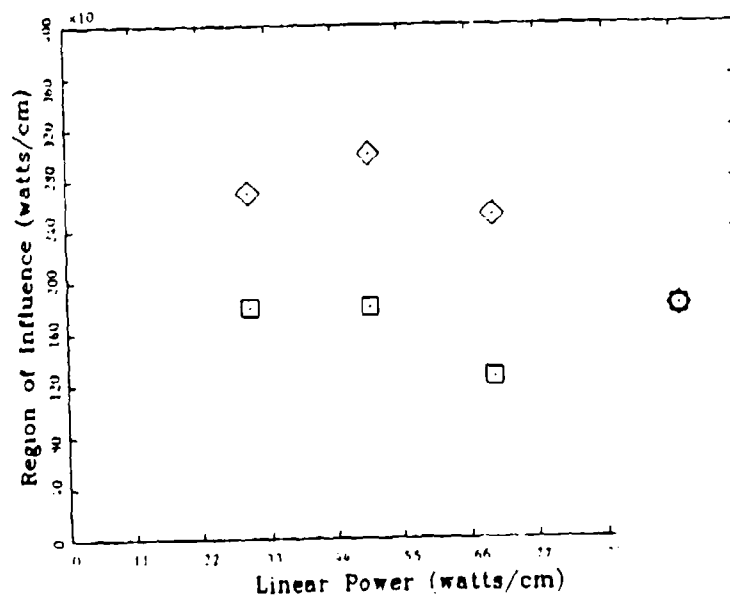


Figure F.30 Region of Influence (W/CM) versus Linear Power
(fuel temp. = 1400 K)

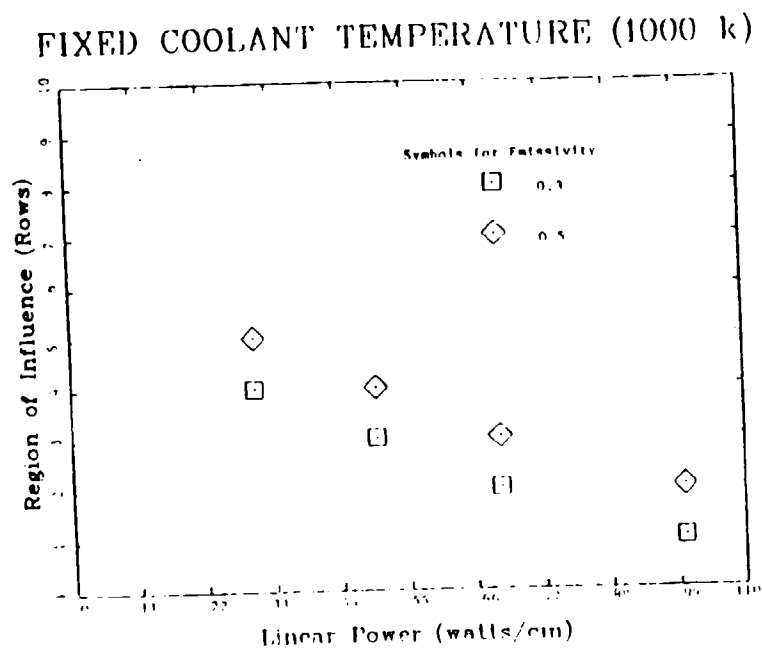


Figure F.31 Region of Influence (Rows) versus Linear Power
(fuel temp. = 1400 K)

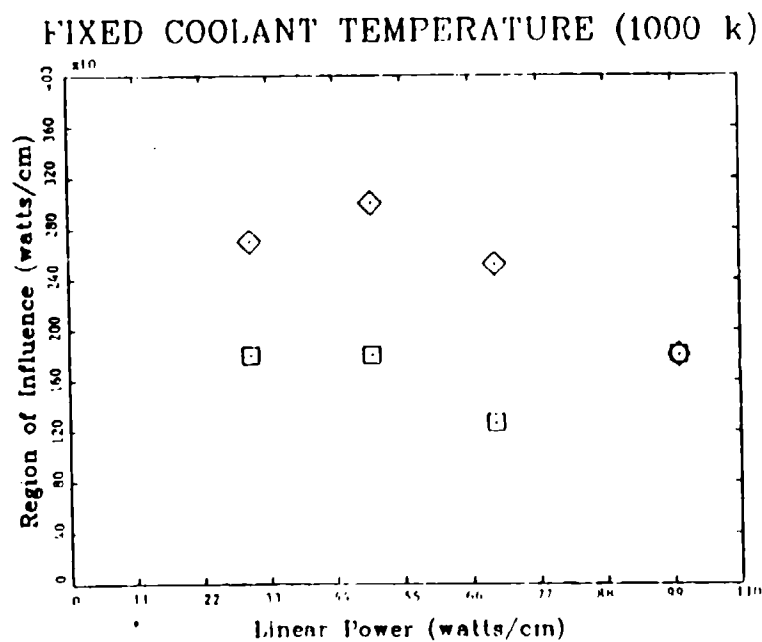


Figure F.32 Region of Influence (W/CM) versus Linear Power
(fuel temp. = 1400 K)

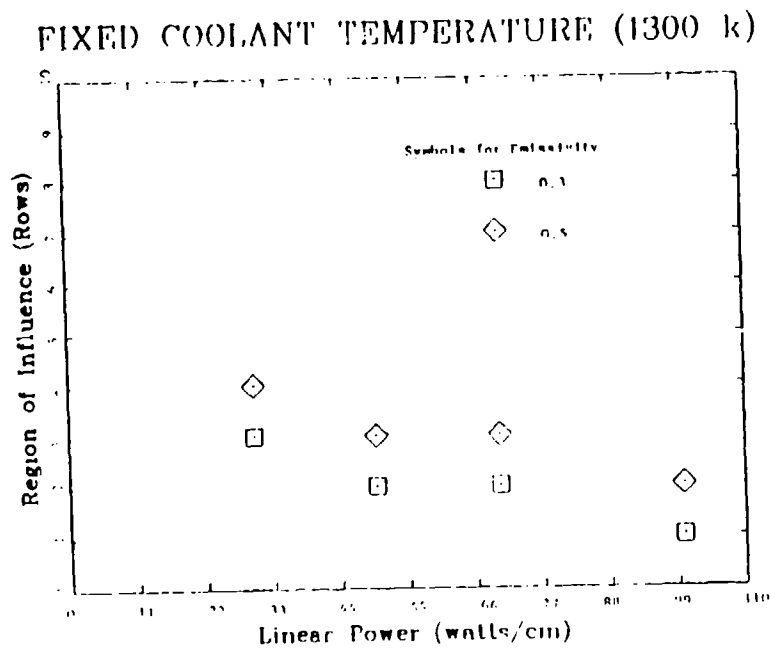


Figure F.33 Region of Influence (Rows) versus Linear Power
(fuel temp. = 1400 K)

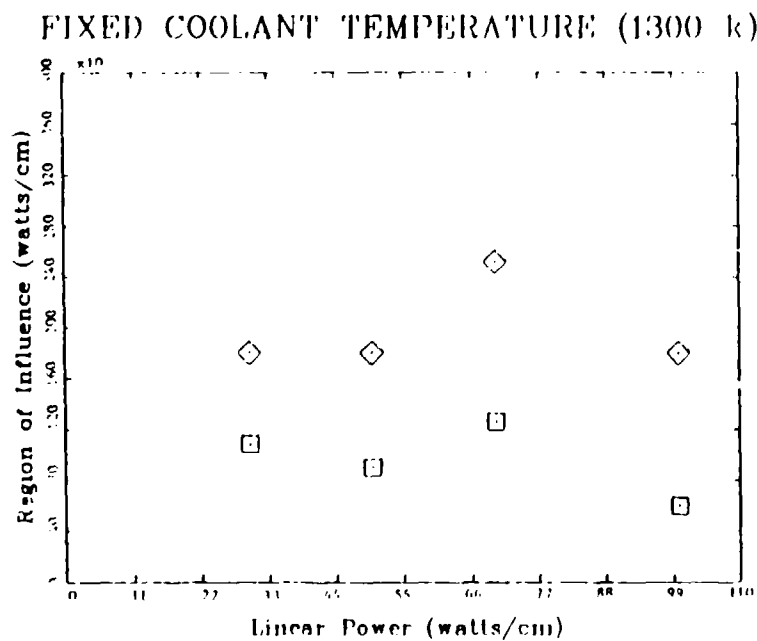


Figure F.34 Region of Influence (W/CM) versus Linear Power
(fuel temp. = 1400 K)

FIXED COOLANT TEMPERATURE (1500 k)

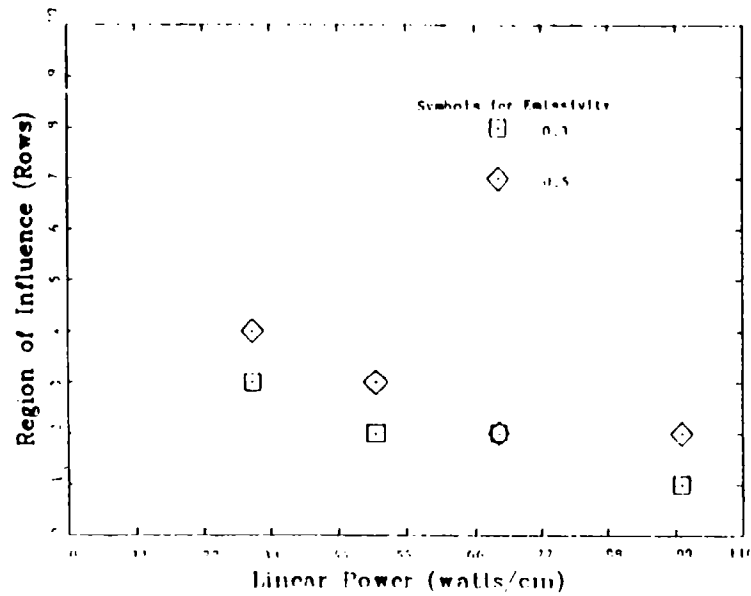


Figure F.35 Region of Influence (Rows) versus Linear Power
(fuel temp. = 1400 K)

FIXED COOLANT TEMPERATURE (1500 k)

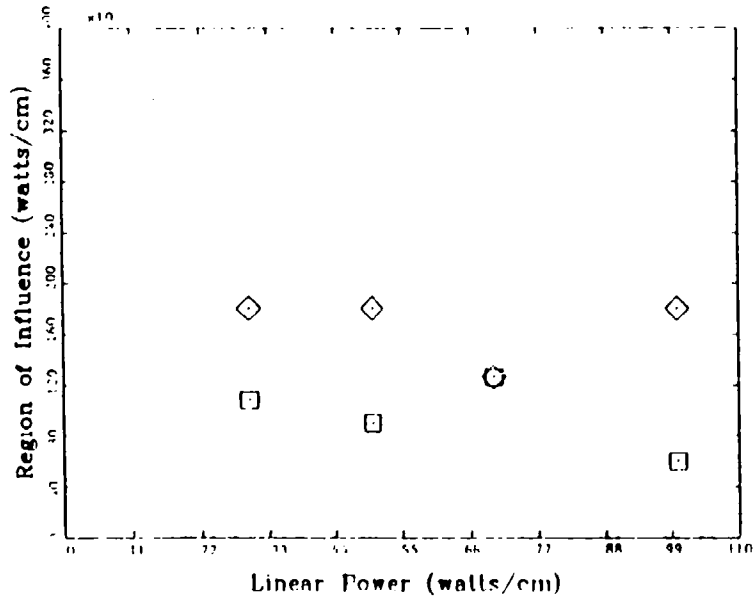


Figure F.36 Region of Influence (W/CM) versus Linear Power
(fuel temp. = 1400 K)

Bibliography

1. Angelo, Joseph A. and David Buden. *Space Nuclear Power*. Florida: Orbit Book Company Incorporated, 1985.
2. Welty, James R. and others. *Fundamentals of Momentum, Heat, and Mass Transfer*. (second edition). New York: John Wiley & Sons Incorporated, 1976.
3. Kreith, Frank *Radiation Heat Transfer for Spacecraft and Solar Power Plant Design*. Scranton PA: International Textbook Company, 1962.
4. Ozisik, M. Necati. *Basic Heat Transfer*. New York: McGraw-Hill, incorporated, 1977.
5. Nakamura, Shoichiro. *Computational Methods in Engineering and Science*. New York: John Wiley and Sons Incorporated, 1977.
6. Adams, Alan L. and David F. Rogers. *Computer-Aided Heat Transfer Analysis*. New York: McGraw-Hill Book Company, 1973.
7. Rust, James H. *Nuclear Power Plant Engineering*. Buchanan, Georgia: Harlson Publishing Company, 1979.
8. Magee, P. M. and others. *Assessment of Loss of Primary Coolant in Orbit*. Report to Los Alamos National Laboratory. Space Nuclear and Energy Technology, General Electric Company, San Jose CA, 6 April 1987.
9. Elson, J. S. "Pin-to-Pin Radiation Heat Transfer Modeling." Memorandum N-12-87-341. Los Alamos National Laboratory, Los Alamos NM, 16 September 1987.
10. Kruger, G. B. "Update-1 to the SP-100 100kWe Core Design." Space Nuclear and Energy Technology, General Electric Company, San Jose CA, 21 May 1987.
11. Biehl, Franz A. "Thermal Analysis Results of Heat-Pipe Concepts for SP-100 Core Coolability." Memorandum N-6-87-737 (B563). Los Alamos National Laboratory, Los Alamos NM, 28 September 1987.

12. Biehl, Franz A. "Results of the Audit Thermal Analysis of the Concept 0 Approach to SP-100 Core Coolability." Memorandum N-8-87-740 (B562). Los Alamos National Laboratory, Los Alamos NM, 28 September 1987.
13. Biehl, Franz A. "Results of a Detailed Thermal Analysis of the Proposed Safety Rod Cooling Approach For the SP-100 Core Cooling Problem." Memorandum N-8-87-740 (B562). Los Alamos National Laboratory, Los Alamos NM, 28 September 1987.
14. Bell, Charles, Project Director. Telephone Interview. Los Alamos National Laboratory, Los Alamos NM, 27 July 1987.
15. ---. Telephone Interview. Los Alamos National Laboratory, Los Alamos NM, 3 August 1987.
16. Biehl, Franz, Project Engineer. Telephone Interview. Los Alamos National Laboratory, Los Alamos NM, 3 August 1987.
17. ---. Telephone Interview. Los Alamos National Laboratory, Los Alamos NM, 11 October 1987.
18. Elson, Jay, Project Engineer. Telephone Interview. Los Alamos National Laboratory, Los Alamos NM, 12 November 1987.
19. Kao, T. "Thermal Systems Analysis Program (TSAP)." Version 1.0.1, 1982.

VITA

First Lieutenant Donald W. Robbins was born on 8 February 1955 in Pittsburgh, Pennsylvania. He graduated from high school in Wall Township, New Jersey in 1973 and attended the University of Delaware until 1977 as a double major in Physics and Electrical Engineering. In March 1978, he enlisted in the United States Air Force and served 18 months as an aircraft crew chief at Altus AFB, Oklahoma. At this point he was awarded a new specialty code as an enlisted research engineer. Following this award Lt. Robbins was assigned to the Electronics System Division (ESD) at Hanscom AFB, Massachusetts. While assigned at ESD he was selected as the ESD Outstanding Airman Of The Year and received acceptance into the Airman Education and Commissioning Program. In June of 1982 Lt. Robbins entered the Georgia Institute of Technology where he received the degree of Bachelor of Nuclear Engineering in June 1984. After graduation, he earned a commission in the USAF through Officer Training School. He then served as Assistant Branch Chief for the Advanced Weapons Technology Branch of the Advanced Strategic Missile Systems Directorate of the Ballistic Missile Office, Norton AFB, California. In August 1986 he entered the School of Engineering, Air Force Institute of Technology as a Masters Degree Candidate.

Permanent address: 1202 Bayberry Road

Manasquan, New Jersey 08736